ENCLOSURE 3

THE INFLUENCE OF REDUCED PEAK FIRING PRESSURE ON THE FATIGUE PERFORMANCE OF MODIFIED-AF PISTON SKIRTS AT SAN ONOFRE UNIT 1

JULY 1988

FAILURE ANALYSIS ASSOCIATES

Failure Analysis Associates®

ENGINEERING AND SCIENTIFIC SERVICES
2225 EAST BAYSHORE ROAD, P.O. BOX 51470
PALO ALTO, CALIFORNIA 94303 (415) 856-9400 TELEX 704216

FaAA-PA-R-88-06-15

THE INFLUENCE OF REDUCED PEAK FIRING PRESSURE ON THE FATIGUE PERFORMANCE OF MODIFIED-AF PISTON SKIRTS AT SAN ONOFRE UNIT 1

Purchase Order A1538905

Prepared by

Failure Analysis Associates®, Inc.
2225 East Bayshore Road
Palo Alto, California 94303

Prepared for

Southern California Edison Company
Rosemead, California 91770

July 1988

TABLE OF CONTENTS

1.0 INTRODUCTION

The purpose of this report is to analyze the possibility of crack initiation and growth in the modified-AF piston skirts in the 20 cylinder RV-4 TDI diesel engines at the San Onofre Nuclear Generating Station Unit 1 (SONGS). This type of piston skirt has been observed to crack in the past [1,2], but in engines with a higher brake mean effective pressure (BMEP) than the nominally 142 psig for the San Onofre engines [3]. This report discusses the effects of reduced BMEP on predicted crack behavior, drawing extensively from earlier results for a BMEP of 225 psig [1,2].

In the earlier work [1,2], it was reported that cracks have been observed in the stud boss region of modified-AF piston skirts in diesel engines manufactured by Transamerica DeLaval, Inc. (TDI) for use in emergency standby power at nuclear power plants. Numerous such cracks were observed in the AF piston skirts at the Shoreham Nuclear Power Station, but these cracks did not impair the operation of the engine, because the cracks grew and then stopped growing at a depth of about 1/2 inch.

Failure Analysis Associates®, Inc. (FaAA) performed an analysis of these piston skirts, with the results reported in References 1 and 2. It was observed that the cracks initiated and grew due to cyclic loading imposed by the firing pressure in the combustion chamber, but that the cracks did not extend beyond a depth of about 1/2 inch. A finite element stress analysis and an experimental strain gage study was performed to determine the stresses in the piston skirt during operation of the engine. The results of the stress analysis and strain measurements agreed well with one another and were used in conjunction with fatigue analyses and fracture mechanics to analyze the initiation and subsequent growth/arrest of these cracks. Good agreement was observed between predicted and observed crack behavior. Determination of the stresses during operation required consideration of the interaction between the piston skirt and the crown, including the effects of thermal distortion of the crown due to nonuniform crown temperature during steady-state operation of the engine. Similar procedures are employed in this report to analyze the behavior of cracks in the modified-AF piston skirts under reduced firing pressure. An additional result not reported before is the crack size as a function of the number of firing cycles once fatigue crack growth threshold conditions have been exceeded. This provides information on the rate at which the crack approaches its final arrested depth.

2.0 REVIEW OF PAST ANALYSES

A review of past analyses [1,2] will be provided here for the sake of completeness.

2.1 Description of Piston Skirt and Crown and Observation of Cracking in Skirt

The piston in a TDI R-4 (or RV-4) engine is composed of a nodular cast iron skirt and a cast steel crown. The crown is attached to the skirt by four studs, with a stack of belleville washers on the studs. Figure 2-1 provides a photograph of the crown and skirt, showing the four attachment studs. Cracking was observed at the stud attachment region of the skirt in the vicinity indicated in Figure 2-2. Figure 2-3 shows a close-up of the stud attachment region with a crack that is made more visible by the use of dye penetrant. As discussed in Reference 1, cracks such as shown in Figure 2-3 were broken open in the laboratory and subjected to microscopic examination. This examination revealed that the cracks had grown due to fatigue loading. None of the cracks grew to the point that they impaired the serviceability of the piston skirts. The piston skirts are fabricated from ASTM A536 nodular cast iron. The microstructure and composition were measured and, as reported in Section 2 of Reference 1, the observations were consistent with this material. Hardness and tensile properties were also measured [1], with the measurements indicating that the material was Grade 100-70-03.

Figure 2-4 schematically shows the piston crown and the upper end of the skirt, along with one of the four attachment studs. As shown in this figure, there is a gap between the crown and the skirt at the outer edge. This gap is specified by TDI to be between 0.007 and 0.011 inch (7-11 mils). The contact between the crown and skirt upon assembly is around the inner contact ring, which is also the ring at which the four crown-to-skirt attachment studs are located. As discussed in Section 2.3, the initial gap at the outer ring can be closed during operation of the engine by the firing pressure in the combustion chamber (pressure at top of crown) and/or thermal distortion of the crown due to nonuniform crown temperatures during engine operation.

2.2 Results of Stress Analysis

Stress analyses were performed using finite elements. Independently of the finite elements, experimental measurements based on brittle lacquer (to show the region of maximum strain) and strain gages (to measure the strain) were made. The stress analyses and measurements were made for uniform pressure on the top of the crown, with compensation then made to account for inertia loading, gap closure, thermal distortion of the crown, and possible lift-off between the crown and skirt due to inertia.

2.2.1 Load Considerations

Gas pressure and reciprocating inertia are the major loads on the piston assembly. The peak gas pressure is associated with the firing pressure in the combustion chamber. A peak firing pressure of 1670 psig was used in earlier analyses, which was for engines with a BMEP of 225 psig. This peak firing pressure was taken to occur at top dead center (TDC) of the power stroke.

The magnitude of the pressure load is obtained knowing the peak firing pressure and cylinder bore (17 inches). A value of 379,000 pounds is obtained for a BMEP of 225 psig. This load is transmitted from the crown to the skirt through the inner and outer contact rings. At top dead center of the power stroke, the pressure load is somewhat offset by the inertia load, which is exerted by the crown to the top of the skirt. The piston acceleration at top center was calculated to be 26.1×10^3 in/sec^2. The crown weighs 144 pounds. Therefore, the inertia force is $144 \times 26.1 \times 10^3/386.4 = 9727$ pounds. Subtracting this from the pressure force provides the maximum net force on the top of the skirt, 369,300 pounds. This corresponds to an effective pressure of 1627 psig. This pressure was applied to the top of the crown for evaluation of the stresses in the piston skirt due to firing pressure.

The other extreme of the stress cycle in the skirt occurs at top center of the exhaust stroke, at which time a tensile load equal to the inertia force of the crown is applied to the top of the skirt. Provided no gap opens between the crown and skirt at the inner ring, the peak stress under this condition is proportional to the pressure loading, and can be obtained from the results for peak firing pressure by multiplying by -9727/369,300 = -0.02634.

The force in the stud induced by assembly was measured by strain gages on the stud and found to be 6600 pounds. The stresses due to this bolt preload were measured and calculated by finite element. The bolt preload was found to have virtually no effect on the stresses in the stud boss region where cracking was observed, and the effects of the bolt preload were omitted from further consideration -- except for situations when the crown separated from the top of the skirt due to inertia loading at TDC of the exhaust stroke. In this situation, the bolt tension load can be an important contributor to the cyclic stress, and it was considered by means discussed in Section 2.3.2.

2.2.2 Stress Analysis

Finite element calculations of stresses in a modified-AF piston skirt were performed by use of the ANSYS Code. The calculations basically consisted of evaluation of stresses in the piston skirt due to an applied pressure on the top of the piston crown. The pressure-induced force was reacted out through a rigid wrist-pin with a vertical load. This corresponds to top dead center. The gap at the outer contact ring was considered not to be closed in the finite element analysis; the effects of gap closure are accounted for by the crown/skirt interaction model discussed in Section 2.3.

The finite element analysis was performed by first analyzing an overall model of the piston and skirt. This model was referred to as the global model and is shown in Figure 2-5. Only one-quarter of the piston needs to be analyzed because of the symmetry of the problem. The global model had 1746 nodes. The second step of the finite element analysis consisted of analyzing a local model of the stud boss region of the piston skirt. The boundary conditions for the local model were drawn from the results for the global model. The local model provided much more geometrical detail in the region of concern and therefore provided more accurate stresses. Figure 2-6 shows the local finite element model, which consisted of 1021 nodes.

Figures 2-7 and 2-8 provide color schematics of the stress contours on the surface of the global and local models. The largest principal stress (in absolute value) was found to be -92.2 ksi in the stud boss region. This is for an "effective" peak firing pressure (pressure force minus inertia force) of 1627 psig with no closure of the other gap between the crown and skirt. This corresponds to the minimum stress in the stress cycle, which occurs at top dead center of the power stroke. The maximum stress occurs at TDC of the exhaust stroke, and (barring lift-off of the crown from the skirt) is equal to 0.02634 x 92.2 = 2.43 ksi, as was discussed in Section 2.2.1.

Additional finite element runs were performed for loading on the outer ring only and loading only by a tensile load on the stud (with no contact between the crown and skirt). The result for loading on the outer ring only showed that stresses in the stud boss region are virtually independent of loading on the outer ring, being dependent solely on the loading on the inner ring. The finite element results for stud loading provided results for use when crown/skirt lift-off is predicted to occur. The maximum principal stress in the stud boss region when crown lift-off occurs for a stud load of 6600 pounds was calculated to be 17.8 ksi.

The finite element runs also provided information on the stiffness of the crown and skirt, and the extent of gap closure. These results are of use in the crown/skirt interaction model. One of the main features of the gap closure results from the finite element runs was that, even though there was a noticeable angular variation in the deformation of the crown and skirt, the gap width between the crown and the skirt was nearly uniform around the circumference. This has important implications in the development of the crown/skirt interaction model.

Several finite element runs were performed on the crown itself in order to determine its stiffness and thermal distortion. Such results are required for the crown/skirt interaction analysis. The downward displacement of the outer ring of the crown was calculated for a uniform pressure applied to the top of the crown, and the result used to evaluate the crown spring constant due to pressure $k_{c(p)}$.

$$k_{c(p)} = \frac{pA}{\delta_0} = 47.4 \text{ kips/mil}$$

The upward displacement of the outer ring of the crown due to a line load around the circumference of the outer ring was also calculated

$$k_{c(F)} = \frac{F}{\delta_0} = 16.4 \text{ kips/mil}$$

Another aspect of the behavior of the piston assembly is the thermal distortion of the crown due to nonuniform temperatures imposed during engine operation. The crown is made from cast steel to make it better able to withstand the high stresses and temperatures at the top of the piston assembly. Thermal gradients were shown to be confined to the crown, with the piston skirt operating at a relatively low, nearly uniform temperature. The gap at the outer contact ring assists in accommodation of the thermal distortion of the crown. This distortion is denoted as δ_T and is the downward displacement of the outer ring relative to the inner ring caused by the top of the crown being hotter than the bottom. Its calculation requires information on the steady-state temperature distribution in the crown and skirt. As reported in Reference 2, the results of peak temperature measurements as a function of position in the crown was supplied to FaAA by TDI. The measurements were made with "templugs" in an R-4 engine operating at 450 RPM and BMEP of 213 psig. The temperature measurements will be assumed to be applicable to the San Onofre engine, which is a conservative assumption. The calculated value of the thermal distortion was 10.7 mils. This parameter is used in the crown/skirt interaction model discussed in Section 2.3.

2.2.3 Experimental Stress Analysis

Experimental measurements were made on piston skirts subject to static pressure on the top of the crown. These measurements consisted of the use of brittle lacquer to identify the maximum stress location in the stud boss region, and strain gage measurements at the maximum stress location and numerous other locations in the piston skirt. These measurements provided benchmarking of the finite element results, as well as insight into the interaction of the crown and the skirt. The elastic constants used to convert strain to stress were

$$E = 23.6 \times 10^6 \text{ psi}$$
$$\nu = 0.3$$

The strain measurements were made at all four stud boss regions. Single element gages were used because of the limited space in this highly stressed localized region. Figure 2-9 presents the results for the most highly stressed of the four stud boss regions. Measurements were made during three pressurization cycles under increasing and decreasing pressure conditions. In addition one set of values was for a conventionally assembled piston and another set with a 5 mil shim inserted between the crown and skirt at the inner contact ring. The outer edge gap with no shim was measured with feeler gages and varied from 7.5 to 9.5 mils, depending on circumferential position. Figure 2-9 shows a bilinear relation between pressure and strain. This bilinearity is due to closure of the gap at the outer contact ring when the pressure is sufficiently large. The abrupt change in slope provides a clear indication of the gap closing pressure. The reduction in stress due to gap closure is clearly evident, which provides a measure of the "load split", i.e., the sharing of the pressure-induced load between the inner and outer rings.

Strain-pressure measurements were made at numerous other locations on the piston skirt, with the bilinear result being observed with an abrupt slope change at about the same pressure -- independently of gage location. This suggests that the gap closes at the same pressure all the way around the crown. This is consistent with the finite element results, and is suggestive of a relatively simple crown/skirt interaction.

The results of Figure 2-9 can be used to estimate the stresses in the stud boss region, which provides results that can be compared to the finite element results. The stress cannot generally be calculated directly from the strain of a single gage. A strain gage rosette was placed as close as possible to the highly stressed region near one of the stud bosses. This rosette indicated that the stresses in this region are nearly uniaxial, thereby eliminating the need for rosettes in these regions. Hence, the uniaxial stress is simply $E\varepsilon$.

The strain gage results were compensated for gap closure (i.e., results at low pressure were extrapolated to higher pressure) and zero offset, and the stress at 1627 psig estimated. The most highly stressed stud boss at this pressure gave a stress value of -107 ksi, and this is used as the "experimental base line" value. The other three stud bosses were considerately lower stressed, having corresponding values of -44, -45, and -63 ksi [Table 5-1, Ref. 2]. These variations are most likely due to geometrical variations resulting from the hand grinding preparation of stud boss regions in the modified-AF skirts. The value of -107 ksi compares well with the -92.2 ksi from the finite element calculations.

2.3 Crown/Skirt Interaction Model

The crown/skirt interaction model is used to account for two important effects in the operation of the piston assembly; i) closure of the gap due to pressure, with its effect on the load distribution between the inner and outer ring, and ii) thermal distortion of the crown, with its effect on gap closure and the load distribution. Reference 2 provides details on the crown/skirt interaction model, which will be briefly summarized here for completeness.

2.3.1 Power Stroke

Figure 2-10 shows the forces acting on the crown and the skirt at top dead center of the power stroke (the inertia force is included as a reduction in the pressure). F_i and F_o are the total loads on the inner and outer contact rings, respectively. The displacements and forces are related by the spring constants of the skirt by the expression

$$\delta_i = \frac{F_i}{k_i} + \frac{F_o}{k_{oi}}$$

$$\delta_o = \frac{F_o}{k_o} + \frac{F_i}{k_{oi}} \qquad (2\text{-}1)$$

(where the reciprocal theorem of elasticity is used to show that $k_{oi} = k_{oi}$). For simplicity in writing later results, the following definitions are employed

$$\frac{1}{k_i'} = \frac{1}{k_i} - \frac{1}{k_{oi}}$$

$$\frac{1}{k_o'} = \frac{1}{k_o} - \frac{1}{k_{oi}} \qquad (2\text{-}2)$$

Using the above spring constants, force equilibrium and the geometrical relations between displacements provides the desired results, the primary one being the ratio of the load on the outer ring to that in the inner ring

$$\frac{F_o}{F_i} = \frac{pA[\frac{1}{k_{c(p)}} + \frac{1}{k_i'}] + \delta_T - g_o}{pA[\frac{1}{k_{c(F)}} - \frac{1}{k_{c(p)}} + \frac{1}{k_o'}] - \delta_T + g_o} \qquad (2\text{-}3)$$

where g_o is the value of the gap upon assembly (i.e., no pressure or thermal distortion), A is the cross-sectional area of the cylinder bore (227 in^2), and other parameters have already been defined. (A negative value of F_o indicates that gap closure has not occurred.)

The above equation can be used for the two operating conditions of the engine; i) start-up conditions, in which case thermal distortion of the crown is initially zero ($\delta_T = 0$) (this is referred to as isothermal conditions), and ii) steady-state running conditions, in which case the piston assembly has come to thermal equilibrium, and $\delta_T = 10.6$ mils.

Once the "load split", F_o/F_i, is known, the corresponding stress in the stud boss region can be calculated, because the stresses in this region are determined solely by the forces on the inner ring (see Section 2.2.2), and the sum of F_o and F_i is known from force equilibrium and the known pressure, bore area and inertia force. The following expression holds

$$\frac{\sigma_{closure}}{\sigma_{no\ closure}} = \frac{F_i}{F_o + F_i} = \frac{1}{1 + F_o/F_i} \qquad (2\text{-}4)$$

2.3.2 Exhaust Stroke

The analysis to determine whether the crown and skirt separate on the inner ring during the exhaust stroke follows procedures similar to those employed above. Whether or not such "lift-off" occurs has an important influence on the peak tensile stresses during the exhaust stroke. The crown is attached to the skirt by four studs, each of which has a static preload of F_{Bo}. Figure 2-11 shows the forces acting on the crown and skirt, where now a separation of δ_L on the inner load ring is considered. The separation distance, δ_L, is taken to be independent of angular position, which is consistent with the assumption that the loading rings remain parallel to one another.

Once a lift-off distance of δ_L is present, the force in a single stud is given by:

$$F_B = F_{Bo} + k_{sw}\,\delta_L \qquad (2\text{-}5)$$

where k_{sw} is the stiffness of the stud/washer combination.

For the purposes of estimating skirt deformation, assume the bolt loads to be distributed around the inner load circle, and treat the sum of these loads as F_i. The use of the load-displacement relations, force equilibrium, and geometrical relationships between displacements provides the following result

$$\begin{aligned}\delta_L(1+\omega) &= \delta_T - g_o - \frac{\omega}{k_{sw}} F_{Bo} \\ &\quad + F_I \left[\frac{1}{k_{c(F)}} + \frac{1}{k'_o} \right] \qquad (2\text{-}6)\\ \omega &\equiv 4k_{sw} \left[\frac{1}{k_{c(F)}} + \frac{1}{k'_i} + \frac{1}{k'_o} \right]\end{aligned}$$

Positive values of δ_L indicate that lift-off has occurred. If such is the case, then the corresponding stud load, F_B, is calculated, and the corresponding stud boss stress obtained by ratioing the known stress for a 6.6 kip stud load (with lift-off). If lift-off has not occurred, then the stress in the stud boss region at TDC of exhaust stroke is obtained by ratioing the results for TDC of the power stroke.

2.3.3 Estimation of Spring Constants

The crown/skirt interaction model presented above contains numerous spring constants. Some of these were evaluated by finite element techniques, as reported in Section 2.2.2. These include the following:

$$k_{c(p)} = 47.4 \text{ kips/mil}$$
$$k_{c(F)} = 16.4 \text{ kips/mil}$$

The stiffness of the stud/washer stack, k_{sw}, was estimated by measuring the stiffness of the washer stack in a test machine (0.15 kips/mil), calculating the stiffness of the stud by elementary strength of materials, and calculating the stiffness of these "springs" in parallel. This provided the following result

$$k_{sw} = \left(\frac{1}{k_{stud}} + \frac{1}{k_w}\right)^{-1} = 0.142 \text{ kips/mil}$$

The remaining spring constants to be determined are k_i' and k_o'. They were evaluated by experimental observations by use of Equations 2-3 and 2-4 knowing the pressure at which the gap just closed ($F_o = 0$) and the "load split" at pressures above gap closure. Both of these effects are shown in Figure 2-9. Another piece of information is the influence of g_o on the gap closure pressure (also shown in Figure 2-9). Using the results shown in Figure 2-9, along with the results from additional strain gages (as reported in References 1 and 2), the spring constants summarized in Table 2-1 were obtained. Also shown are the corresponding finite element values, which are seen to fall within the range of the values based on experimental observations in conjunction with the crown/skirt interaction model.

2.4 Fatigue Crack Initiation

The pistons experience 1.35 million cycles of stress every 100 hours of operation. Consequently crack initiation under high cycle fatigue conditions is of concern, and the endurance limit of the material is the property of interest. Reference 4, and references cited therein, indicate that a lower bound on the endurance limit of cast iron with the properties of the 100-70-03 material used in the skirt is 30 ksi. The endurance limit is applicable to fully reversed uniaxial stress (zero mean stress). In order to perform a fatigue analysis on the piston skirt, the non-zero mean stress must be accounted for. This is accomplished by use of a Goodman diagram, such as shown in Figure 2-12. Figure 2-13 shows the definition of the the terms employed.

Once the ultimate strength (σ_{ult}), endurance limit (σ_n), and yield strength (σ_{ys}) are known, the conditions for infinite fatigue life are defined. If the mean stress (σ_m) and stress amplitude (σ_a) fall outside the truncated triangle of Figure 2-12, then crack initiation is predicted to eventually occur. As reported in Reference 1, the measured yield strength of AF piston skirt material fell within the range of 53.6 to 64.5 ksi. The following set of properties are used to construct the Goodman diagram

$$\sigma_{ys} = \begin{matrix} 53.6 \text{ ksi} & \text{min.} \\ 64.5 \text{ ksi} & \text{max.} \end{matrix}$$

$$\sigma_{ult} = 100 \text{ ksi}$$

$$\sigma_n = 30 \text{ ksi}$$

2.5 Crack Propagation

Earlier analyses [1,2] of fatigue crack growth used a fatigue crack growth threshold (ΔK_{th}) of 6.4 ksi-in$^{1/2}$ at R (=K_{min}/K_{max}) of 0. The fatigue crack growth rate (da/dN) for a given ΔK (K_{max}-K_{min}) at R = 0 was taken to be

$$\frac{da}{dN} = 2.47 \times 10^{-12} \Delta K^{5.15} \qquad (2\text{-}7)$$

where da/dN is in inches/cycle and ΔK is ksi-in$^{1/2}$. The influence of R on da/dN (for a given ΔK) was treated by use of the Hop-Rau formulation in the BIGIF Code [5]. Since the earlier analyses were not concerned with the crack size as a function of the number of cycles since initiation, accuracy of the da/dN-relation near threshold was not of concern. In the current study, it is desired to determine the crack size versus number of cycles, and greater care in the growth rate relations near threshold is desired. Procedures for more accurately describing these characteristics are included in Section 3.2.

The fracture toughness of the skirt material was taken to be 40 ksi-in$^{1/2}$, and this value will be used here.

The elastically calculated stresses due to the peak firing pressure, as reported in Section 2.2, are sufficient to cause yielding in the stud boss region of the AF skirt. Residual tensile stresses are predicted in the localized region where the stresses exceed the yield strength. The contained plasticity capability in BIGIF [5] was used to obtain the elastic-plastic redistributed stress field. The elastic-plastic redistributed stresses had a substantial tensile component that can cause cracks to grow. These tensile components result from an upward shift in the mean stress due to yielding caused by the high compressive stresses under peak firing pressure.

The stress intensity factor range, ΔK, due to the plastically redistributed cyclic stresses was calculated using BIGIF [5]. The crack was idealized as a plane strain crack in a strip of finite width. Values of ΔK, as calculated using BIGIF, were compared to the threshold value for crack growth, ΔK_{th}, at the defined stress ratio, R.

3.0 EXTENSION TO SAN ONOFRE ENGINES

The stresses and the crown/skirt interaction model discussed in Sections 2.2 and 2.3 are used to analyze the initiation and growth in the stud boss region of the modified-AF piston skirts in the engines at San Onofre Unit 1 by procedures outlined in Sections 2.4 and 2.5 -- once adjustments in stress levels due to reduced BMEP are made. Additionally, since the crack size versus cycles since initiation is now of specific interest, alterations to the crack growth relation are called for.

3.1 Stresses for Reduced BMEP

The cyclic stresses in the piston skirts will be reduced below that considered earlier, because the peak firing pressure is lower for reduced BMEP.

3.1.1 Peak Firing Pressure for Reduced BMEP

Earlier stress analyses were performed for a BMEP of 225 psig, which had a corresponding peak firing pressure of 1670 psig. The San Onofre engines are called upon to operate at a steady BMEP of 142 psig during surveillance testing and initially during an emergency load event, and at 65 psig BMEP later in an emergency load event [3]. The peak firing pressure in the range of 65 - 142 psig BMEP is therefore of interest. The necessary information is available from the factory test logs of the San Onofre Unit 1 Engines [6]. Table 3-1 summarizes the pertinent data from the logs. This data is plotted in Figure 3-1, which also shows the following straight line fit

$$p_f = 400 + 5.2\ (\text{BEMP}) \tag{3-1}$$

(where all pressures are in psig). This provides the following peak firing pressures and corresponding "effective" peak firing pressures for the two BMEP values of interest

BMEP	p_f	Effective p_f
65	738	695
142	1138	1095

These results are useful in the scaling of the cyclic stresses.

3.1.2 Cyclic Stresses for Reduced BMEP

The cyclic stresses for various conditions can now be calculated for the two BMEP values of interest. Results are presented for the following conditions

- finite element base line stress and experimental base line stress (-92.2 and -107 ksi at 1627 psig effective)
- gaps of 7 and 11 mils
- BMEP of 65 and 142 psig (effective p_f = 695 and 1095 psi)
- isothermal and steady-state operation conditions ($\delta_T = 0$ and 10.6 mils)
- minimum and maximum of values of skirt spring constants

  ($k_i' = 25.8$, $k_o' = 8.0$ and $k_i' = 83.7$, $k_o' = \infty$ kips/mil)

Table 3-2 summarizes the results and the procedure used to obtain them.

3.2 Fatigue Crack Growth Properties

Since the number of cycles required to grow a crack to a given size once it has initiated is desired in the current analysis, a more careful characterization of the fatigue crack growth properties just above the threshold is required. This is accomplished by use of the modified Forman relation [7], which has been proposed since the work reported in References 1 and 2 were originally performed. This relation is the following

$$\frac{da}{dN} = C(1-R)^m \, \Delta K^n \, \frac{[\Delta K-(1-C_0 R)^d \, \Delta K_{th}]^p}{[K_c-(1-R) \, \Delta K]^q} \tag{3-2}$$

The constant m is typically taken as zero. C_0 and d control the effect of R on threshold conditions, and were taken as 0.578 and 1 (respectively) to be consistent with the Hop-Rau formulation used in earlier work [1,2]. As discussed in Section 2.5, ΔK_{th} and K_c were 6.4 and 40 ksi-in$^{1/2}$ in earlier work, and these values will be retained here. The sum n+p is the slope of da/dN-ΔK on log-log paper at intermediate crack growth rates, and this sum will be taken to be 5.15 to be in accordance with earlier work (see Equation 2-7). The constant p controls the curvative of the da/dN-ΔK relation as threshold conditions are approached from above. A value of p of 1/2 was selected, based on comparisons with data on near-threshold conditions for fatigue crack growth in nodular cast iron as reported in Reference 8. This value is typical for a wide variety of ferrous materials, as reported in Reference 9. The constants p and q are generally taken to be equal [9], and this will be done here. Finally, the value of C was selected in order to provide (approximate) agreement with Equation 2-7 in the intermediate crack growth range. This provides a value of C of 1.34×10^{-11} (for da/dN is inches/cycles and ΔK is ksi-in$^{1/2}$). This provides the following end result

$$\frac{da}{dN} = 1.34 \times 10^{-11} \, \Delta K^{4.65} \left\{ \frac{\Delta K-(1-0.578R)6.4}{40-(1-R)\Delta K} \right\}^{1/2} \tag{3-3}$$

Figure 3-2 provides a plot of da/dN - ΔK for R=0 for the new relation (Equation 3-3) and the older relation (Equation 2-7).

4.0 RESULTS

The cyclic stress, fatigue, and fracture mechanics properties reviewed in the previous sections will now be applied to the analysis of crack initiation and growth in the stud boss region of the modified-AF piston skirts in the San Onofre Unit 1 Engines.

4.1 Crack Initiation

The values of σ_{min} and σ_{max} for various conditions are summarized in Table 3-2. Converting the values to σ_m and σ_a, then plotting on a Goodman diagram such as shown in Figure 2-12, provides the results shown in Figures 4-1 and 4-2. These two figures are for the two BMEP levels of interest. Two Goodman diagrams are shown; one for the minimum reported yield strength (53.6 ksi) and one for the maximum reported yield strength (64.5 ksi).

Figure 4-1 shows that at a BMEP of 142 psig cracks may or may not initiate under isothermal conditions, depending primarily on the value of the yield strength assumed. If the conservative minimum yield strength is employed, cracks are predicted to initiate under isothermal conditions. In contrast to this, cracks are predicted not to initiate under steady-state operating conditions. Figure 4-2 shows that at a BMEP of 65 psig cracks are predicted not to initiate.

The results of Figure 4-1 predict that cracks may initiate in the stud boss region of the modified-AF piston skirts. Since the cracks are growing into a decreasing stress field, they may or may not grow and may or may not be subsequently arrested. Questions of subsequent growth and arrest are addressed by a fracture mechanics analysis.

4.2 Crack Propagation

Whether or not an initiated fatigue crack will grow under subsequent loading is determined by a fracture mechanics analysis. This analysis requires the stress gradient into the stud boss in order to determine the stress intensity factors as a function of crack depth. This gradient is available only from the finite element analysis, and is shown in Figure 4-3 for the minimum and maximum of the stress cycle. The elastically calculated stresses locally exceed the yield strength of the material. The material will consequently yield, which will locally redistribute the stresses. For earlier analyses the redistributed stresses were calculated using the contained plasticity capability contained in the BIGIF Code [5], which is based on the procedures in Reference 10. These procedures have been incorporated into the NASCRAC™ Code [11,12], which was used for the determination of the redistributed stresses employed in the current work. The NASCRAC™ Code was also used for the analysis of crack growth, because this newer code provides the capability to easily employ the modified Forman crack growth relation used for the more accurate representation of near-threshold fatigue crack growth properties.

Figure 4-3 also shows the redistributed minimum and maximum stresses based on the NASCRAC Code calculations using the minimum reported yield strength. It is seen that the stress redistribution significantly shifts the mean stress to a more tensile value. Once the stresses have been redistributed due to the large compressive stresses induced by isothermal operation, the stresses under steady loading may or may not grow the crack. If lift-off between the crown and skirt occurs, then a larger tensile stress is imposed which may be detrimental to crack growth. Figure 4-3 also shows cyclic steady-state stresses as a function of depth for a gap of 7 mils and maximum spring constants.

The σ_{min} and σ_{max} versus depth results for isothermal and steady-state stress conditions shown in Figure 4-3 are used to calculate K_{max} and K_{min} as a function of crack depth. This is accomplished by use of the NASCRAC™ Code [11,12], which performs the calculations in the same manner as the BIGIF Code [5] used in the earlier work. Crack sizes for exceedance of threshold (a_i) and arrest conditions (a_a) are calculated along with crack size as a function of the number of stress cycles (since exceedance of threshold). Table 4-1 summarizes the results. This table shows that crack growth can occur only

---

NASCRAC is a trademark of Failure Analysis Associates, Inc.

under a very restricted set of unfavorable conditions, which include simultaneous minimum gap size (7 mils) with maximum spring constants. Under these particular conditions, the crown is predicted to lift-off from the top of the skirt. This increases the tensile stress at the σ_{max} conditions, thereby providing conditions under which cracks are predicted to grow. However, in all instances, cracks are predicted to arrest at a depth of less than 0.477 inch, so failure of the piston skirt is <u>not</u> predicted to occur. The predicted crack arrest depths are comparable to those observed in the Shoreham pistons [1], and predicted by earlier analyses [1,2].

The crack depth as a function of operating time is presented in Figures 4-4 and 4-5 for the particular unfavorable situations in which any crack extension whatever is predicted to occur. These two figures provide results for the finite element base line and experimental base line stresses, respectively. Results are presented in these figures for combinations of load profiles consisting of the following

1. Twenty 2-hour surveillance tests at steady load at BMEP = 142 psig.

2. One emergency load event: 0 - 10 hrs. at BMEP = 142 psig; 10 hrs. - 7 days at BMEP = 65 psig.

These load profiles are based on information from Southern California Edison [3] and represent bounds on future operation of the engines. In each of Figures 4-4 and 4-5, three sets of results are presented

i. Steady operation at BMEP = 142 psig.

ii. Twenty 2-hour surveillance tests at BMEP = 142 psig followed by emergency load with 10 hours at BMEP = 142 psig, followed by 7 days at BMEP = 65 psig.

iii. No surveillance testing, an emergency load event with 10 hours at BMEP = 142 psig, followed by 7 days at BMEP = 65 psig.

Scenarios ii and iii correspond to transferring to the 65 psig curve at 50 hours and 10 hours respectively. The above three scenarios bracket the future operation of the engine (except for the possibility of 0 hours at 142 and 7 days at 65).

Figures 4-4 and 4-5 provide crack depths as a function of time following exceedance of fatigue crack growth threshold conditions and can therefore be thought of as conservative estimates of crack size under future operating conditions, given that an observable crack is not now present. These figures therefore represent a conservative estimate of possible crack size in the stud boss regions during future operation, following an inspection in which no cracks are observed.

Although Figures 4-4 and 4-5 show considerably different results in many respects, they invariably show that cracks will arrest at depths less than 0.477 inch. Furthermore if the future time spent at 142 BMEP is less than 10 hours, the cracks in the stud boss region will be no deeper than about 40 mils. If the full 50 hours at 142 BMEP is accumulated, then the crack depth at the maximum expected future operating time is at about 1/2 to 1 times the fully arrested crack depth, depending on whether the finite element or experimental base line stresses are employed in the analysis. Consequently, the limited future operation of the engines cannot be said conservatively to have a significant influence on predicted crack sizes; roughly the same sizes would be present if the future hours of operation were not restricted. However, it must be recalled that the cracks are predicted to grow at all only for a very restricted set of conditions, and the many conservativisms included in the analysis should be remembered.

5.0 SUMMARY AND CONCLUSIONS

The purpose of this report is to analyze the possibility of crack initiation and growth in the modified-AF piston skirts in the 20-cylinder RV-4 TDI diesel engines at the San Onofre Nuclear Generating Station Unit 1. This type of piston skirt has been observed to crack in the past, but in engines with a higher brake mean effective pressure (BMEP). This report addresses the effect of the reduced BMEP rating of the San Onofre engines and the fairly short desired remaining operating time of these piston skirts.

The effects of reduced BMEP and short projected remaining service usage are addressed by use of the stress analysis and fracture mechanics analysis performed previously on modified-AF piston skirts for the TDI Diesel Generator Owners Group by Failure Analysis Associates, Inc.. Adjustments and additions to earlier work are made to compensate for lower BMEP and to provide a more accurate description of fatigue crack growth in the near-threshold region.

After making the compensation and adjustments, it was found that cracks are predicted to initiate in the highly stressed stud boss region of the modified-AF piston skirts in the San Onofre engines for outer ring gaps within the TDI-specified range of 7-11 mils. However, these cracks will propagate only under a very restricted set of conditions, and any cracks that are predicted to propagate are also predicted to arrest at depths less than 0.477 inch. These conclusions are very similar to earlier ones for engines with a higher BMEP, except that the conditions for possible growth are more restricted, and the arrested depths are somewhat less.

Calculations of crack depth as a function of time following exceedance of threshold conditions showed that at 142 BMEP cracks approached their arrest depths in times of about 50-100 hours. However, if the engine was considered to operate at 65 BMEP after some hours at 142, crack depths considerably less than the final arrest depth may be expected, but (under worst case conditions) the limited remaining operating time expected for these piston skirts does not result in predicted crack depths substantially less then the final arrested depth at very long times. This is under worst case combination of conditions, and it should be recalled that under most combinations of conditions that crack propagation is predicted to not occur at all.

6.0 REFERENCES

1. "Investigation of Types AF and AE Piston Skirts," Failure Analysis Associates Report FaAA 84-2-14 to TDI Diesel Generator Owner's Group, Palo Alto, California, May 23, 1984.

2. "The Influence of Thermal Distortion on the Fatigue Performance of AF and AE Piston Skirts," Failure Analysis Associates Report FaAA 84-5-18 to TDI Diesel Generator Owner's Group, Palo Alto, California, June 1984.

3. Letter from David F. Pilmer, Southern California Edison Company, to Jerrell M. Thomas, Failure Analysis Associates®, Inc., June 13, 1988.

4. Iron Castings Handbook, edited by C.F. Walton and T.J. Opar, Iron Casting Society, Inc., 1981.

5. P.M. Besuner, et al., "BIGIF -- Fracture Mechanics Code," EPRI Report NP-1830-CCM, Electric Power Research Institute, Palo Alto, California, 1981.

6. Power Engine Factory Test Logs, Engine Numbers 75041 and 75042, for Southern California Edison, DeLaval Engine and Compressor Division, Oakland, California, 1976.

7. R.G. Forman and T. Hu, "Application of Fracture Mechanics on the Space Shuttle," Damage Tolerance in Metallic Structures, ASTM STP 847, Philadelphia, Pennsylvania, 1984, pp. 108-133.

8. F.D. Griswold, Jr. and R.I. Stephens, "Comparison of Fatigue Properties of Nodular Cast Iron Production and Y-Block Castings," International Journal of Fatigue, Vol. 9, No. 1, 1987, pp. 3-10.

9. R.G. Forman, et al., "Fatigue Crack Growth Computer Program -- NASA/FLAGRO," Lyndon B. Johnson Space Center JSC-22267, Houston, Texas, 1986.

10. P.M. Besuner and S.A. Rau, "Stress and Subcritical Crack Growth Analysis Under Contained Plastic Conditions," Electric Power Research Institute Report NP-81-8-LD, Palo Alto, California, 1981.

11. D.O. Harris, et al., "NASCRAC -- A Computer Code for Fracture Mechanics Analysis of Crack Growth," Paper AIAA-87-0847-CP, 28th Structures, Structural Dynamics and Materials Conference, 1987.

12. "NASCRAC™ -- NASA CRack Analysis Code," Draft User's Manual, Version 1.20, Failure Analysis Associates®, Inc., Palo Alto, California, May 1988.

Table 2-1
Summary of Experimental Observations Related to Crown/Skirt Interaction in AF Piston Skirts With Corresponding Stiffnesses

	Nominal	Minimum	Maximum
Initial gap, g_o, mils	8.0	7.5	9.5
Gap closure pressure, psig	800	700	1000
$\sigma_{closure}/\sigma_{no\ closure}$ at 1670 psig	0.80	0.75	0.92
k_i', kips/mil	44.4	25.8	83.7
k_o', kips/mil	31.9	8.0	∞
Finite element, k_i', kips/mil	82.1		
Finite element, k_o', kips/mil	116		

Table 3-1

Peak Firing Pressure for Various BMEP From the San Onofre Unit 1 Engine Factory Test Logs [6]

(All pressures in psig)

BMEP	Engine 75041			Engine 75042		
	Min	Max	Ave	Min	Max	Ave
39	--	--	--	530	550	540
77	710	780	752	630	660	642
116	720	780	755	890	930	907
116	--	--	--	870	920	894
154	1080	1210	1151	1080	1180	1126

Table 3-2

Summary of Stresses for Various Conditions

(All stresses in ksi, all pressure in psig, all displacements in mils)

	Finite Element Base Line				Experimental Base Line			
σ_{III} @ 1627 psig (no closure) σ_{max} = -0.026 σ_{III} (no lift-off) (§ 2.2.1)	-92.2 (§ 2.2.2) 2.43				-107 (§ 2.2.3) 2.82			
Gap, g_o, mils	7		11		7		11	
Spring Constants	Min k	Max k	Min k	Max k	Min k	Max k	Min k	Max k
BMEP = 142: σ_{min} (no closure) (linear with eff p_f)	-62.0	-62.0	-62.0	-62.0	-72.0	-72.0	-72.0	-72.0
BMEP = 142, Isothermal: Load split, F_o/F_i (Eq. 2-3)	0.1642	0.0718	0.0746	0	0.1642	0.0718	0.0746	0
σ_{min} (Eq. 2-4)	-53.3	-57.9	-57.7	-62.0	-61.9	-67.2	-67.0	-72.0
σ_{max}	2.43	2.43	2.43	2.43	2.82	2.82	2.82	2.82
BMEP = 142, Steady-State: Load split, F_o/F_i (Eq. 2-3)	0.4943	1.8715	0.3499	0.7577	0.4943	1.8715	0.3499	0.7577
σ_{min} (Eq. 2-4)	-41.9	-21.6	-45.9	-35.3	-48.2	-25.1	-53.3	-41.0
δ_L (Eq. 2-6)	0	2.18	0	0	0	2.18	0	0
σ_{max} (adj. for δ_L if $\delta_L > 0$)	2.43	18.7	2.43	2.43	2.82	21.7	2.82	2.82
BMEP = 65: σ_{min} (no closure)	-39.4	-39.4	-39.4	-39.4	-45.7	-45.7	-45.7	-45.7
BMEP = 65, Isothermal: Load split, F_o/F_i (Eq. 2-3)	0.0743	0	0	0	0.0743	0	0	0
σ_{min} (Eq. 2-4)	-36.7	-39.4	-39.4	-39.4	-42.5	-45.7	-45.7	-45.7
σ_{max}	2.43	2.43	2.43	2.43	2.82	2.82	2.82	2.82
BMEP = 65, Steady-State: Load split, F_o/F_i (Eq. 2-3)	0.5820	3.2746	0.3424	0.7193	0.5820	3.2746	0.3424	0.7193
σ_{min} (Eq. 2-4)	-24.9	-9.22	-29.4	-22.9	-28.9	-10.7	-34.0	-26.6
δ_L (Eq. 2-6)	0	2.18	0	0	0	2.18	0	0
σ_{max} (adj. for δ_L if $\delta_L > 0$)	2.43	18.7	2.43	2.43	2.82	21.7	2.82	2.82

Table 4-1

Summary of Results for Initiation and Arrest Crack Sizes

			Finite Element Base Line				Experimental Base Line			
		Gap, g_o, mils	7		11		7		11	
		Spring Constants	Min k	Max k	Min k	Max K	Min k	Max k	Min k	Max k
BMEP = 142	Isoth.	Crack Initiation a_i, inch a_a, inch		*	*	*	*	*	*	*
BMEP = 142	Steady-State	Crack Initiation Lift-Off a_i, inch a_a, inch		* 0.035 0.441				* 0.024 0.477		
BMEP = 65	Isoth.	Crack Initiation a_i, inch a_a, inch								
BMEP = 65	Steady-State	Crack Initiation Lift-Off a_i, inch a_a, inch		* 0.065 0.441				* 0.034 0.454		

Crack initiation (with min. σ_{ys}), lift-off indicated by an asterisk.

Crack growth predicted only in situations where crack data is provided.

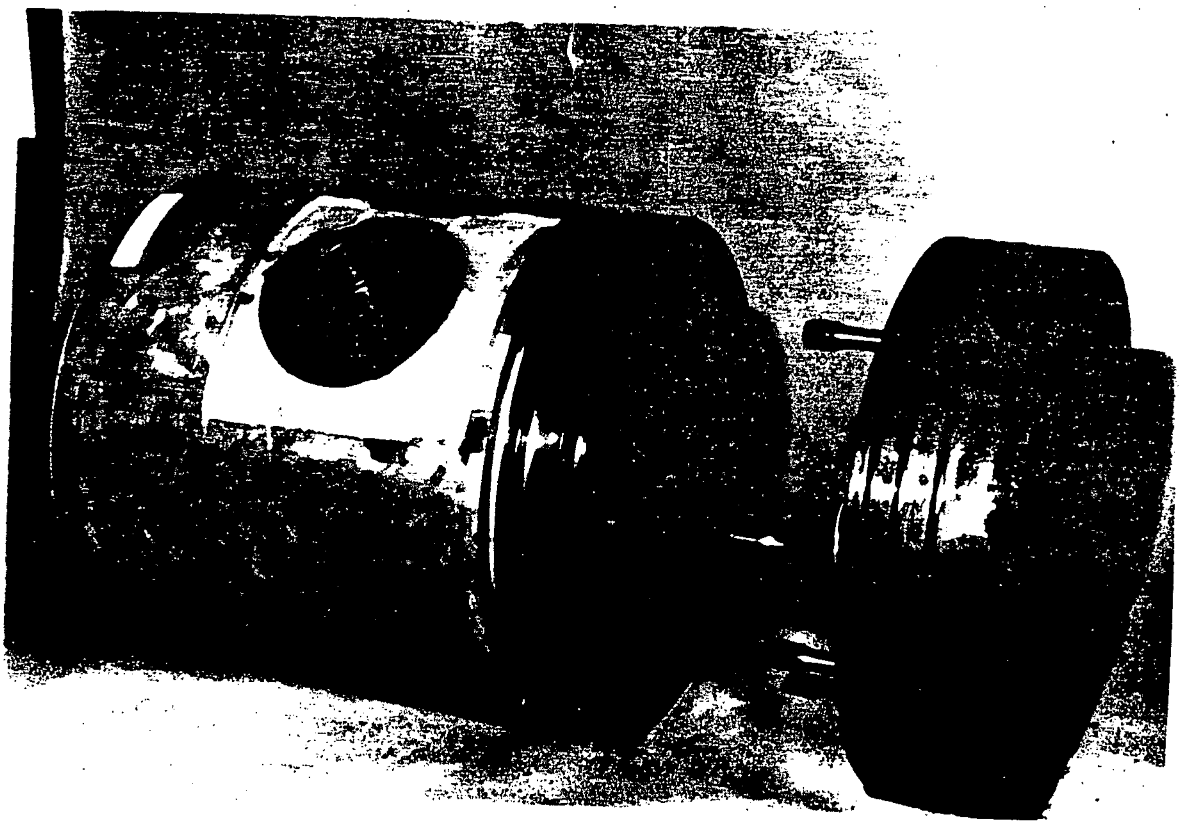

Figure 2-1. Photograph of an AF-type piston from the Shoreham Nuclear Power Station emergency diesel generator piston skirt (left) and crown (right). [Photo Id No.: 03719 #20]

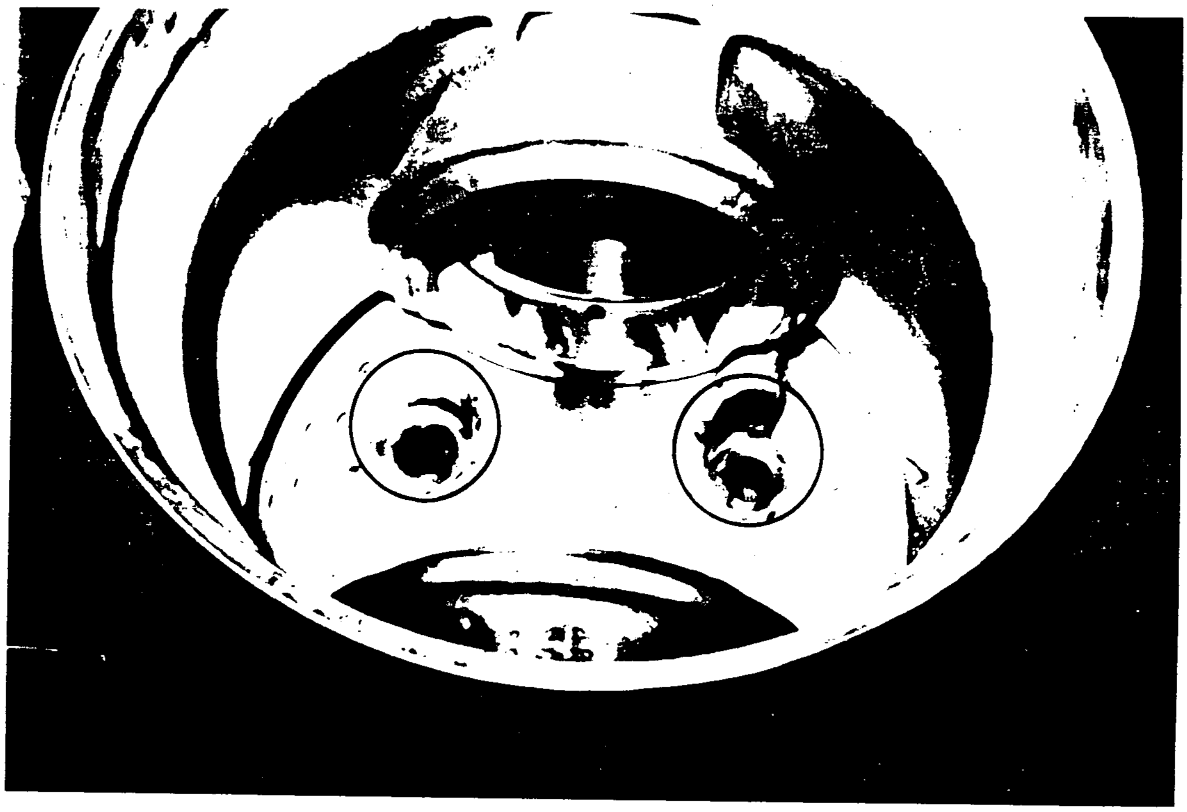

Figure 2-2. Interior of an AF-type piston skirt. The white coating and red dye are from the dye penetrant examination. Through holes for the crown studs and spot-faced boss are circled. [Photo Id No.: 03697 #29]

Figure 2-3. A crown-to-skirt attachment boss from EDG #102. The piston skirt has been tested with red dye penetrant and white developer. A red linear indication is visible at the base of the vertical ridge that remained after spot-facing. [Photo Id No.: 03712 #5]

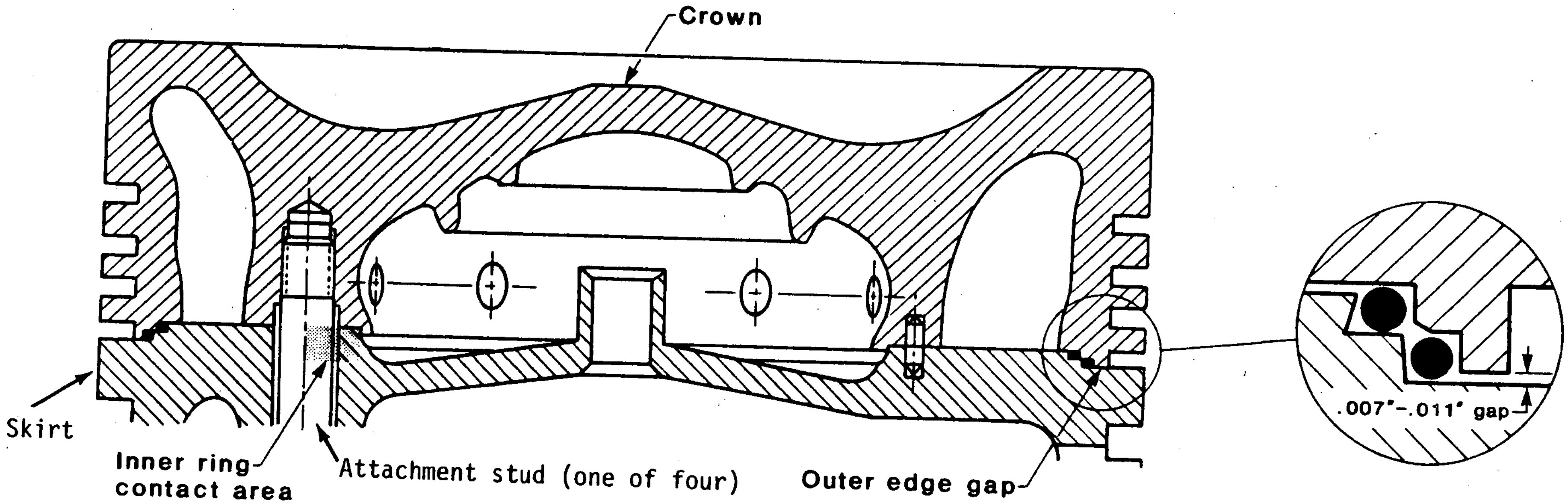

Figure 2-4. Cross section of crown and skirt indicating the two areas of load transfer from the crown to the skirt.

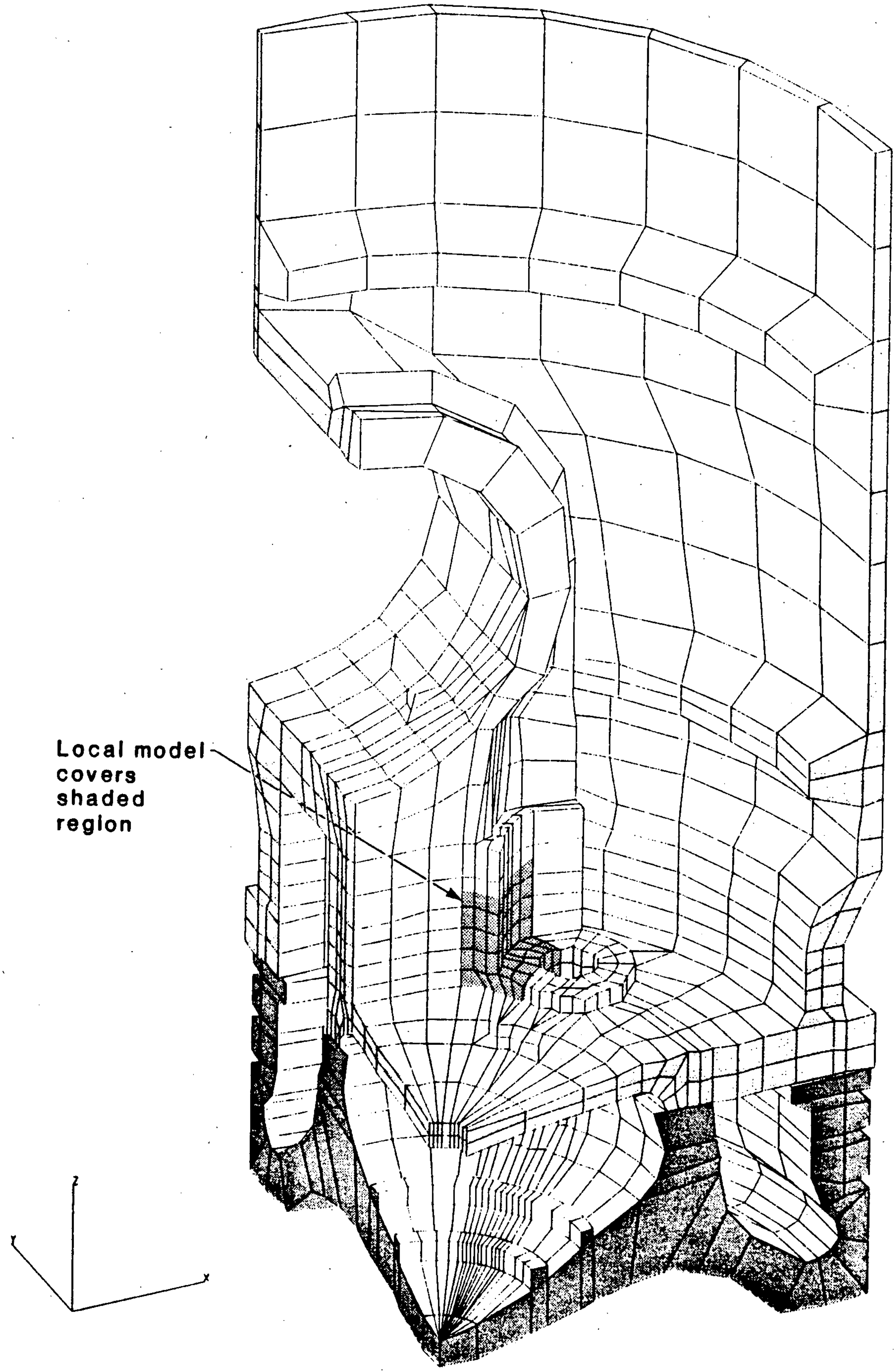

Figure 2-5. AF piston skirt global model with crown.

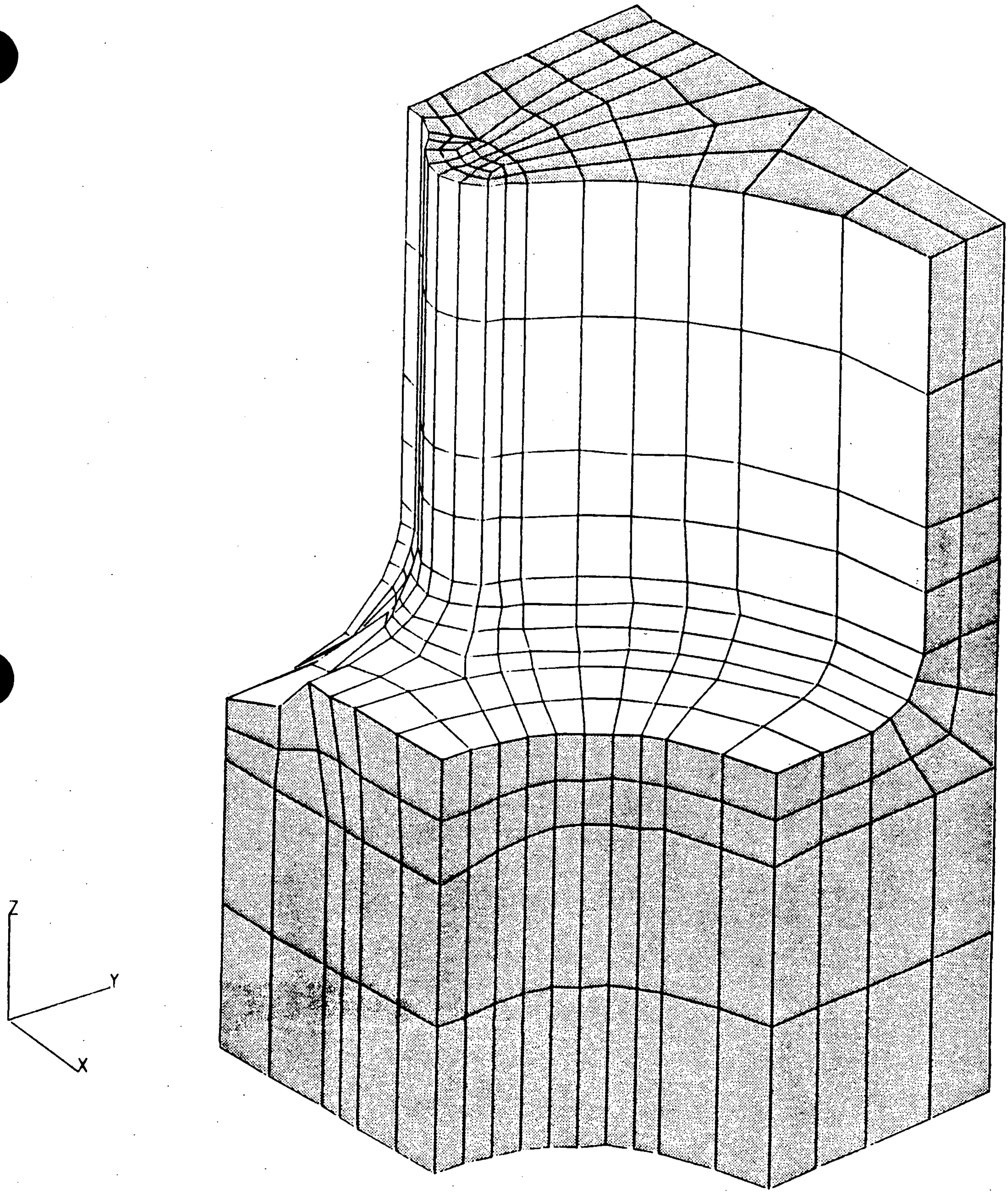

Figure 2-6. AF piston skirt stud-boss local model.

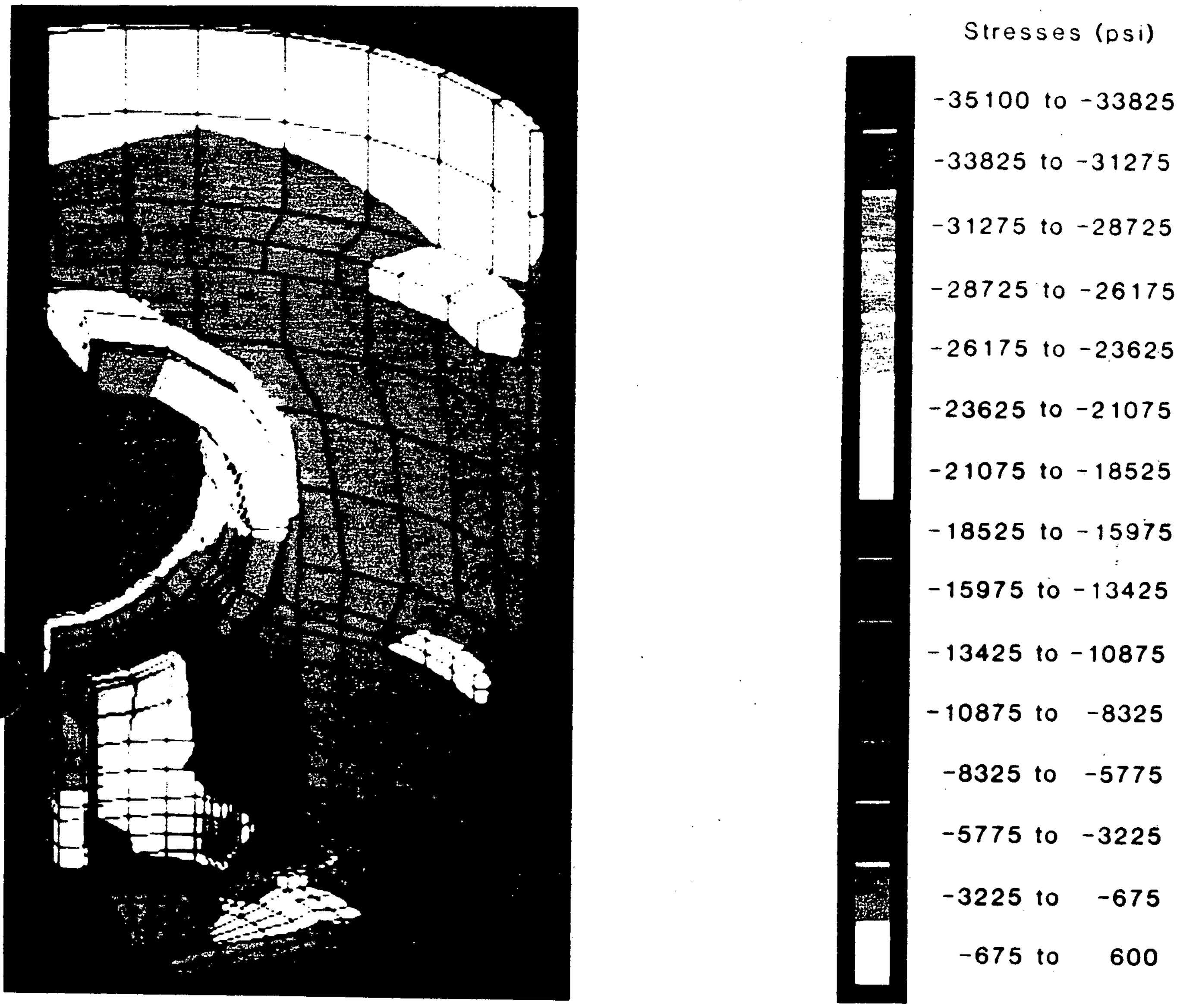

Figure 2-7. AF piston skirt global model with stress contour of average element (σ_{III}) stresses for a skirt with a pressurized crown and no loading on the outer ring.

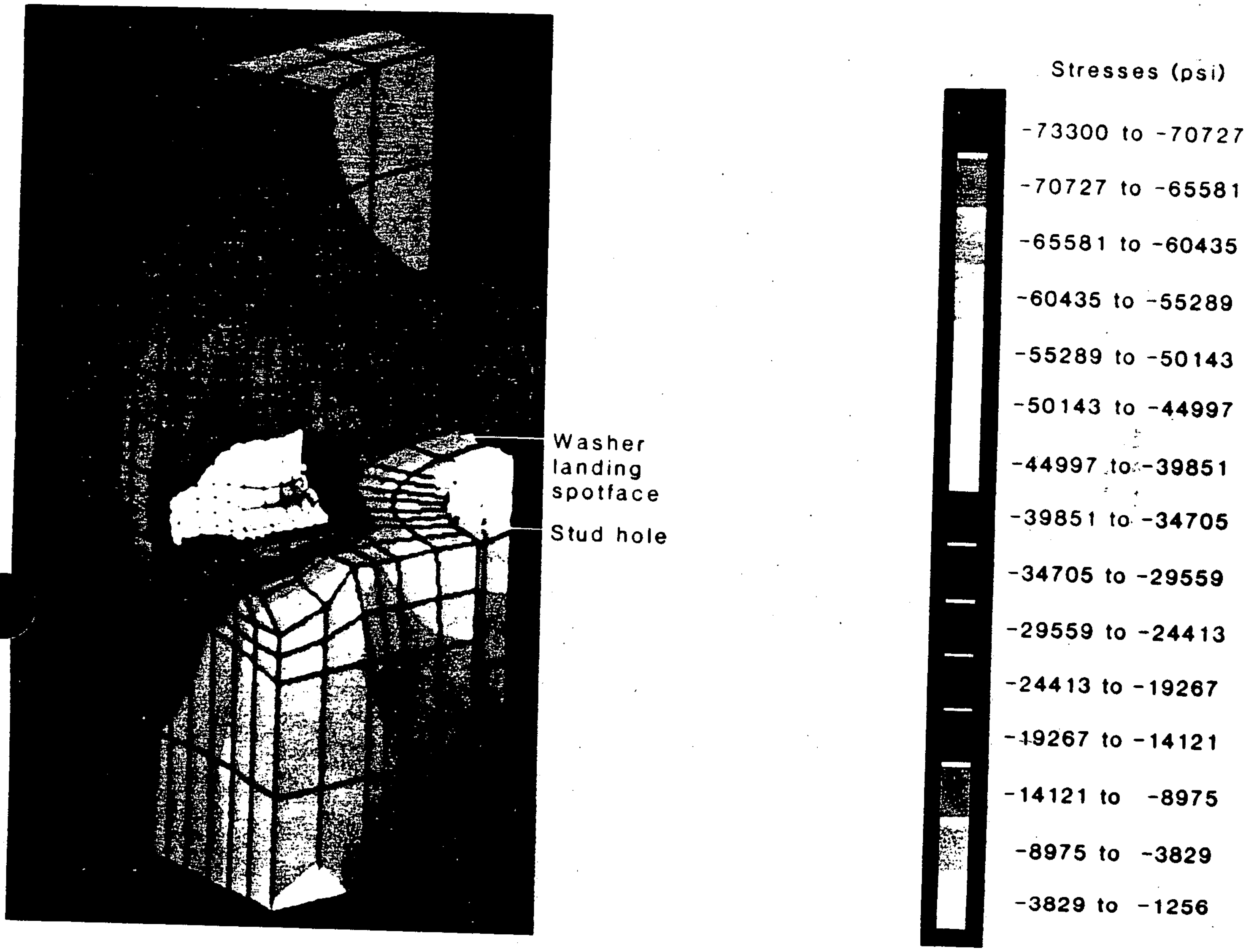

Figure 2-8. AF piston skirt local model with stress contour of average element (σ_{III}) stresses for a skirt with a pressurized crown and no loading on the outer ring.

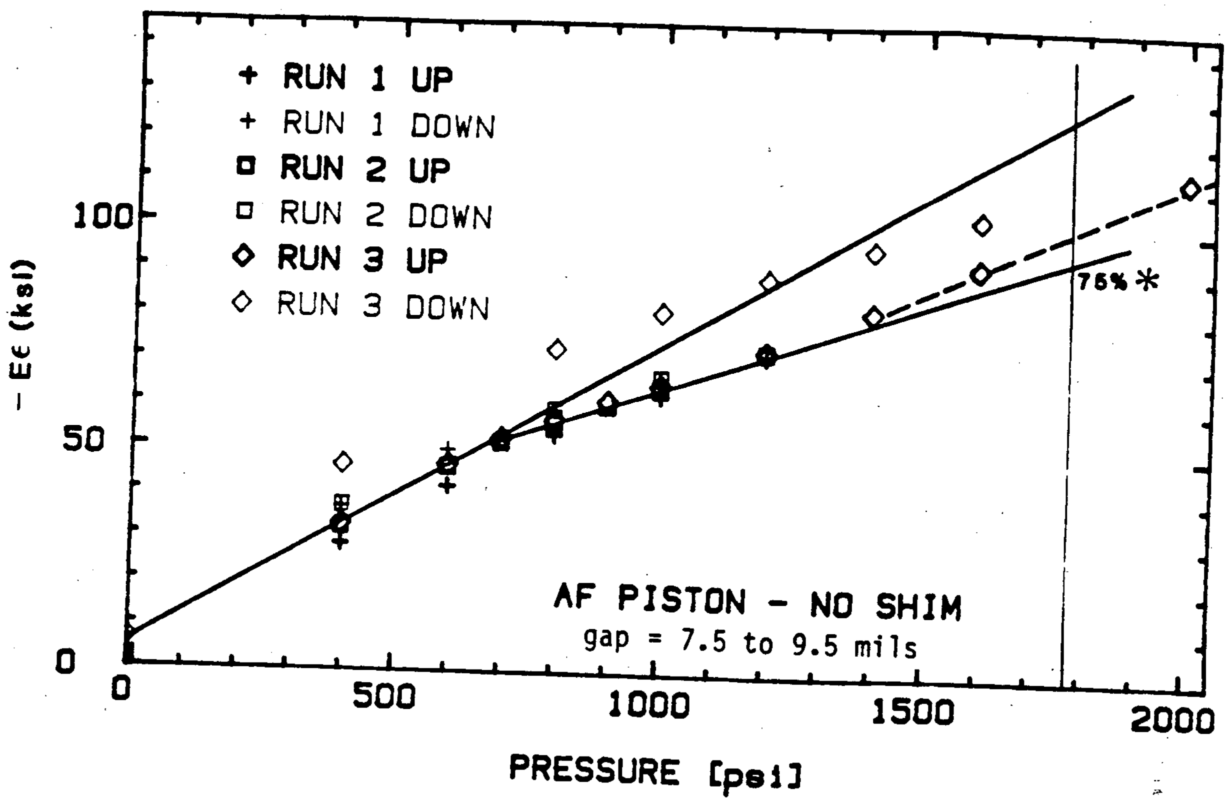

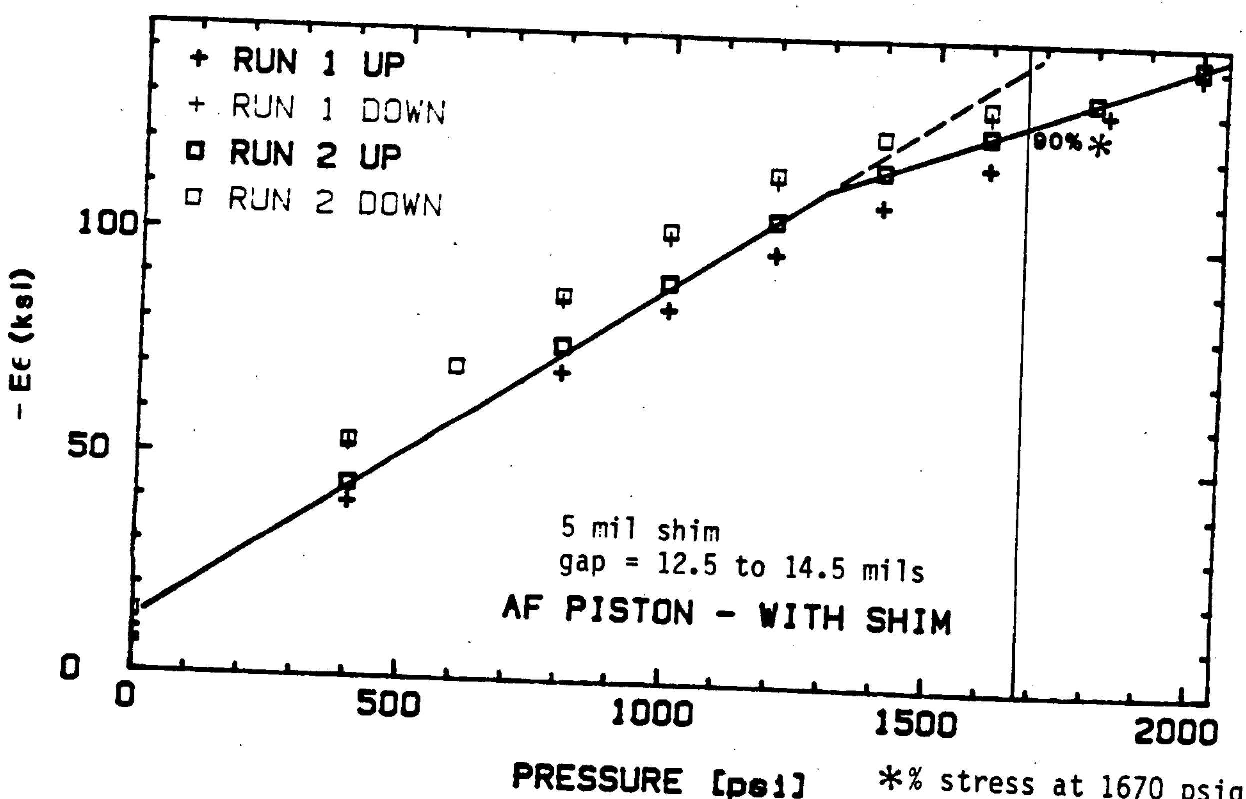

*% stress at 1670 psig reflecting gap closure.

Figure 2-9. Elastically calculated stress as a function of pressure for most highly stressed stud base gage with and without shim.

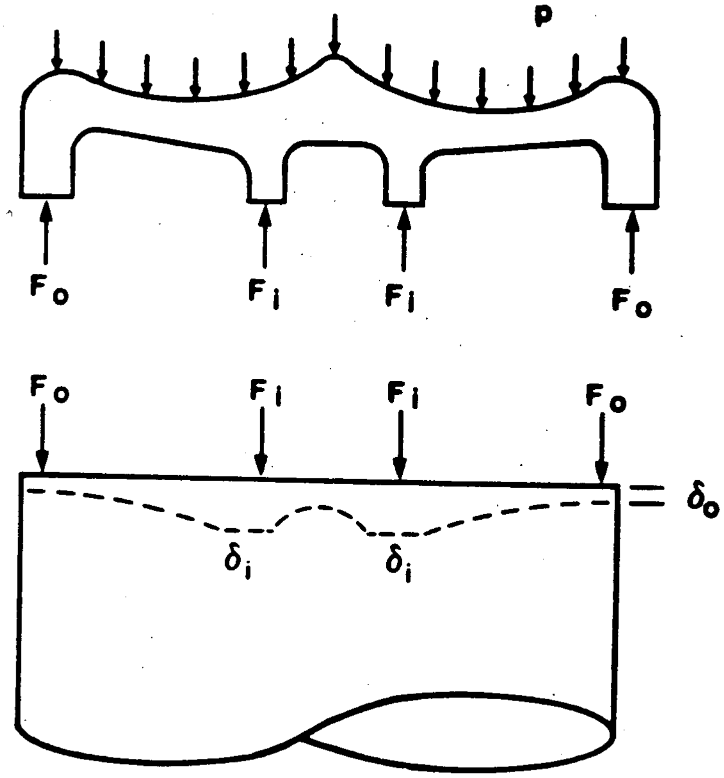

Figure 2-10. Schematic representation of loads and displacements on inner and outer contact rings of crown and skirt.

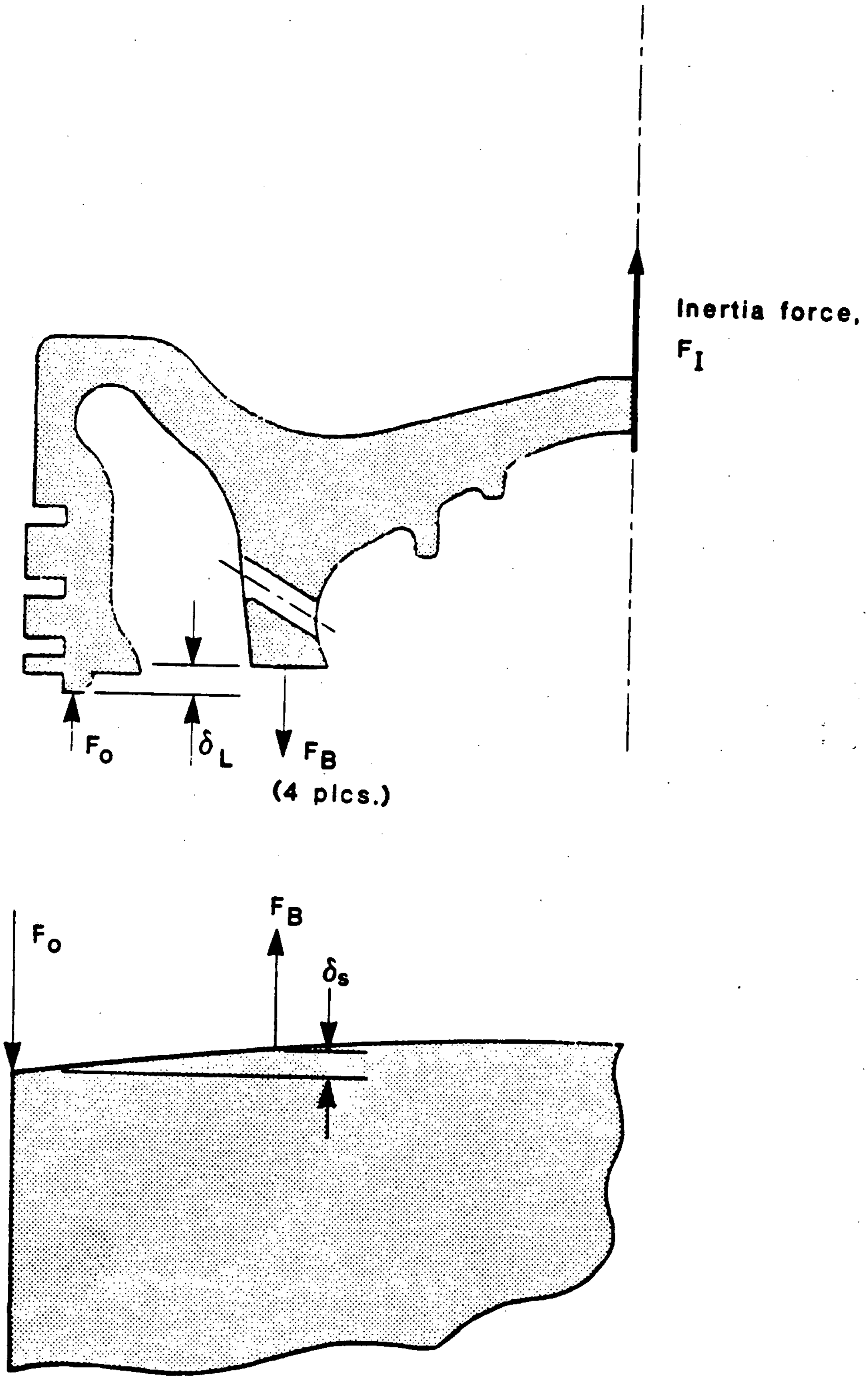

Figure 2-11. Forces acting on crown and skirt at top dead center of exhaust stroke.

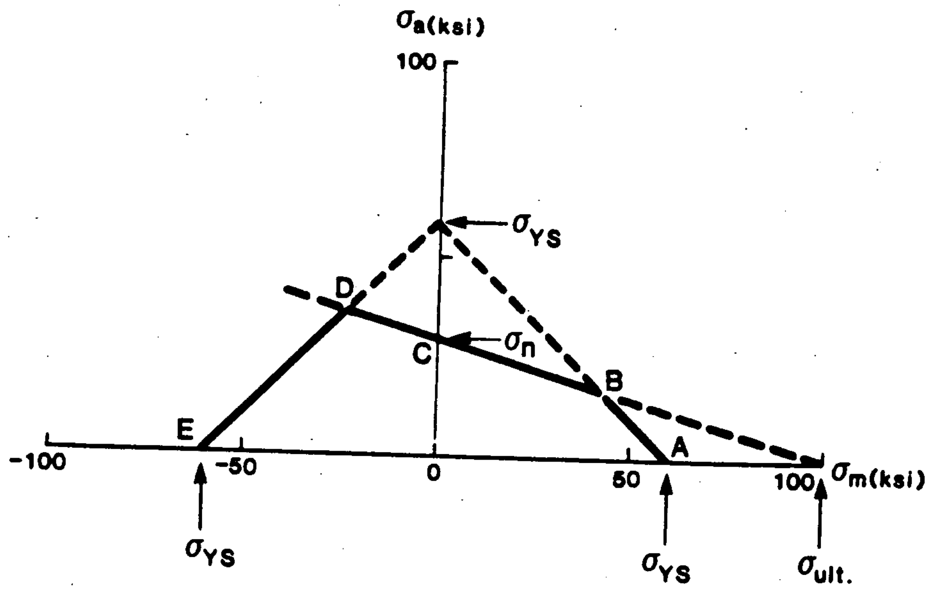

Figure 2-12. Mean and cyclic stresses for infinite fatigue life.

$$\sigma_{mean} = 1/2(\sigma_{max} + \sigma_{min})$$
$$\sigma_a = 1/2(\sigma_{max} - \sigma_{min})$$

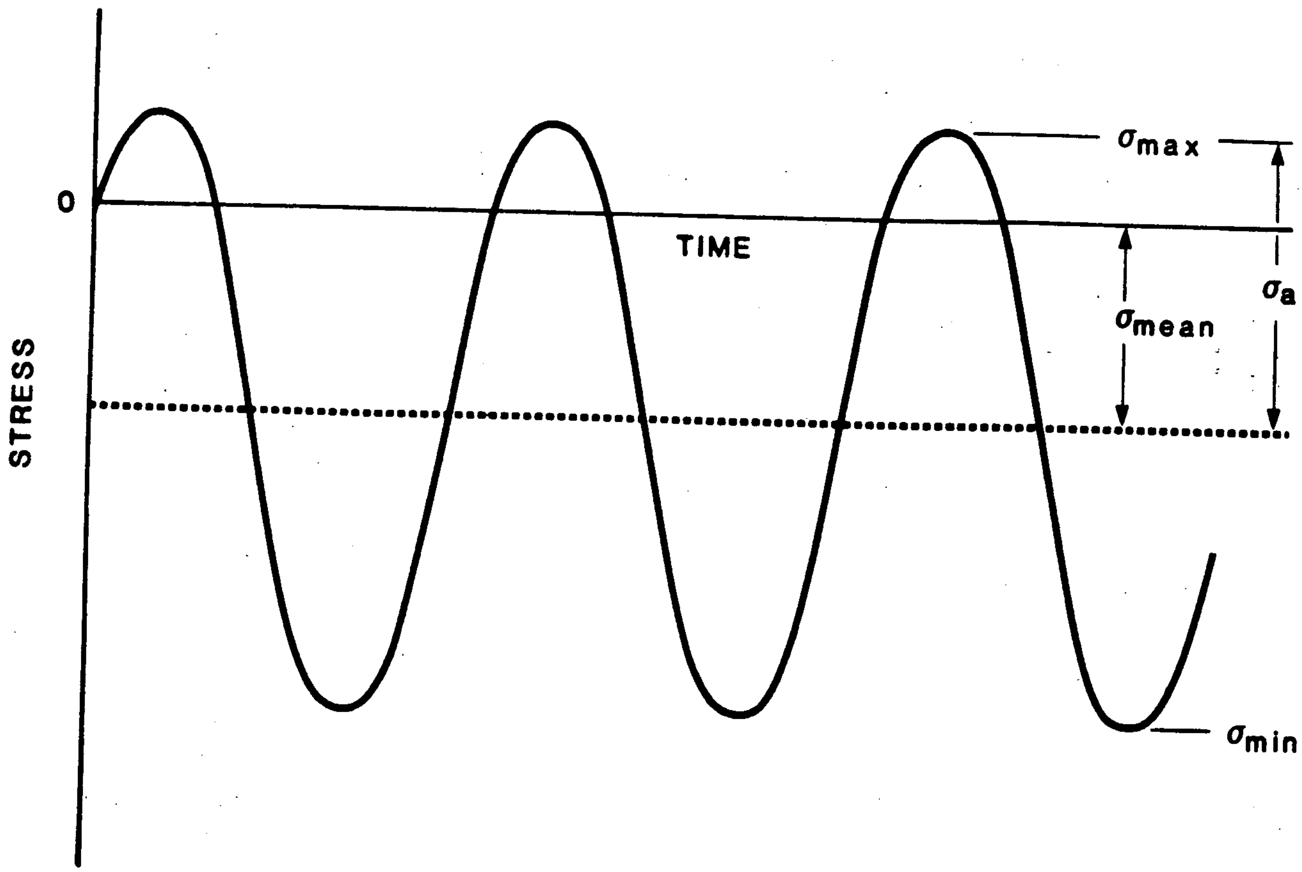

Figure 2-13. Definition of terms for cyclic applied stresses.

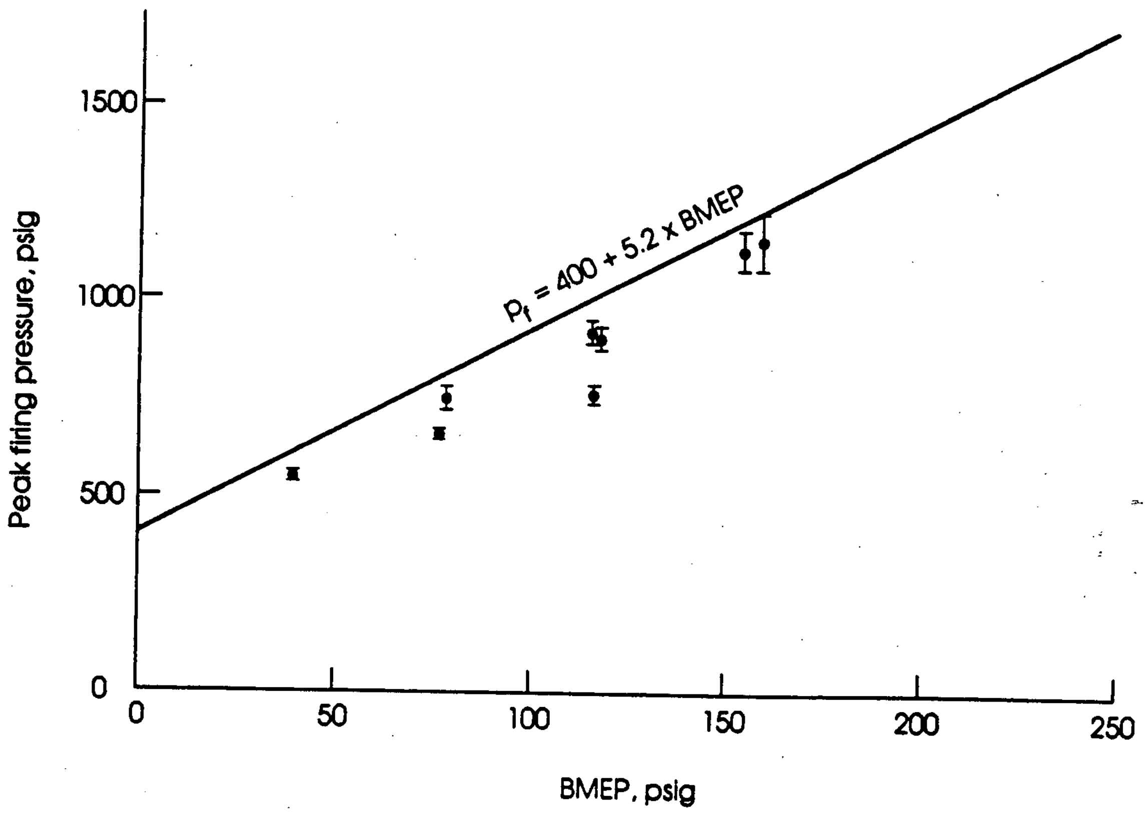

Figure 3-1. Peak firing pressure as a function of BMEP for San Onofre 1 engines (data from Reference 6).

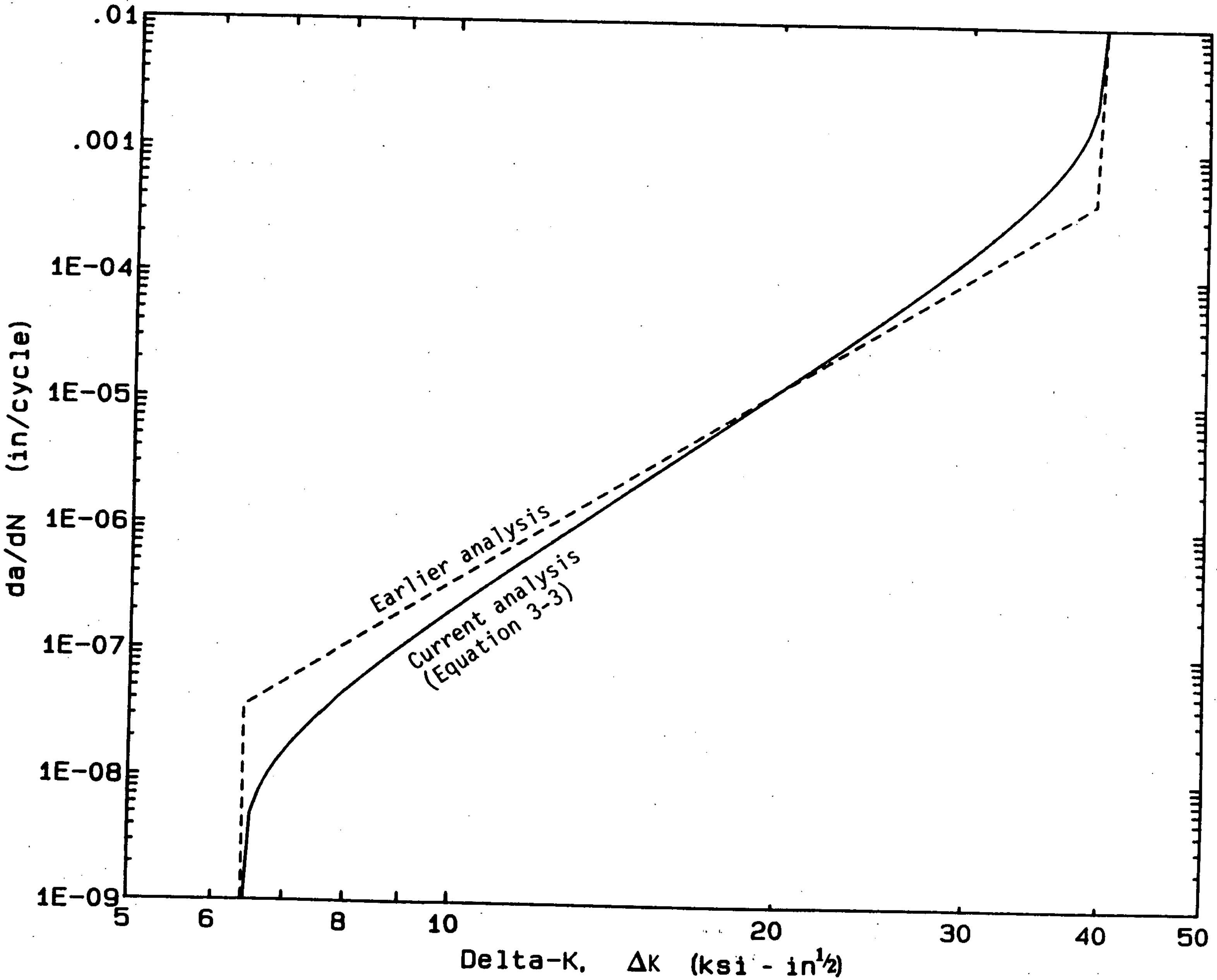

Figure 3-2. Fatigue crack growth relations for earlier and current analyses.

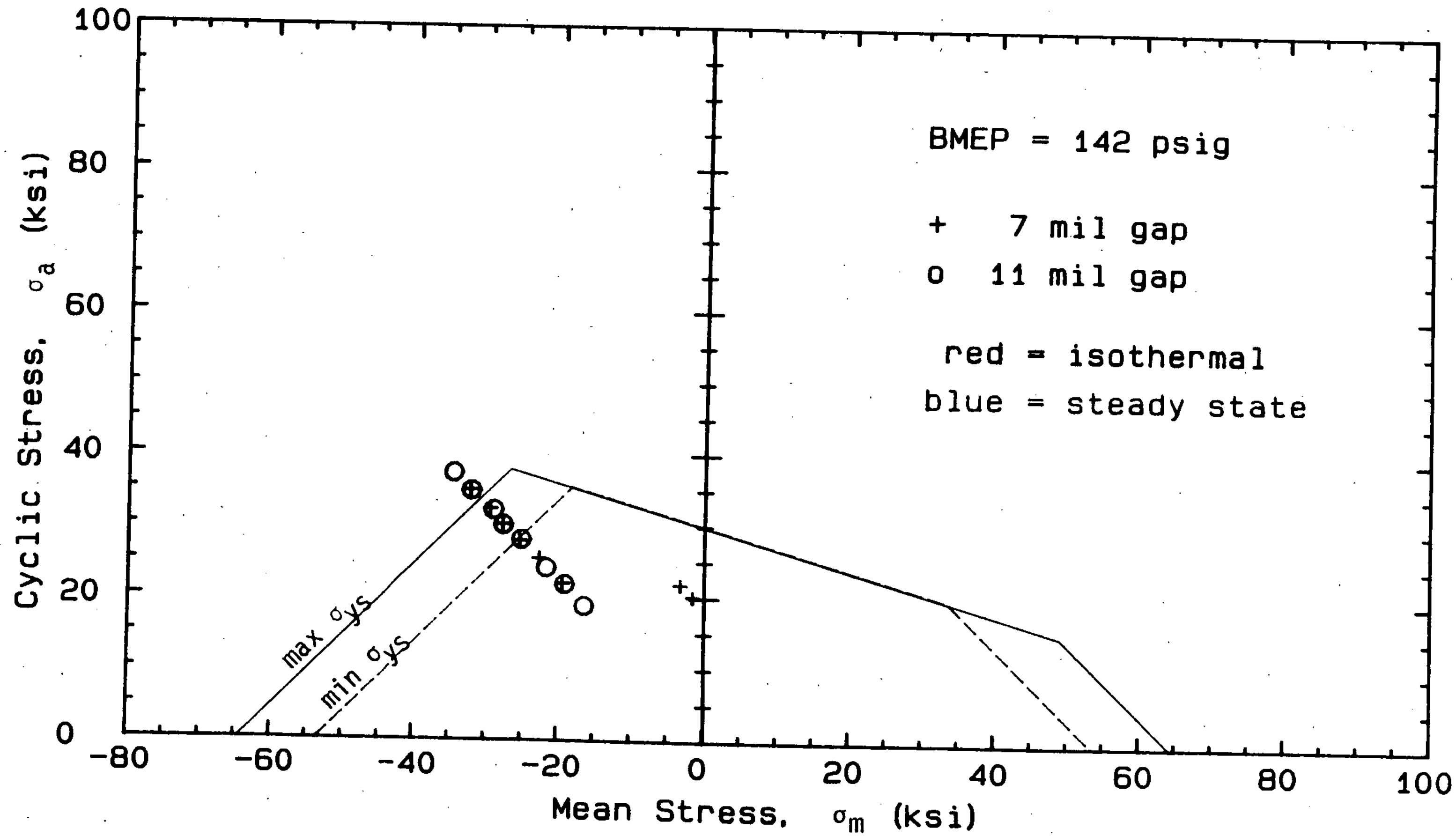

Figure 4-1. Mean and cyclic stresses at BMEP of 142 psig along with Goodman diagram showing that cracks may initiate under certain isothermal conditions. (Both min k and max k results shown.)

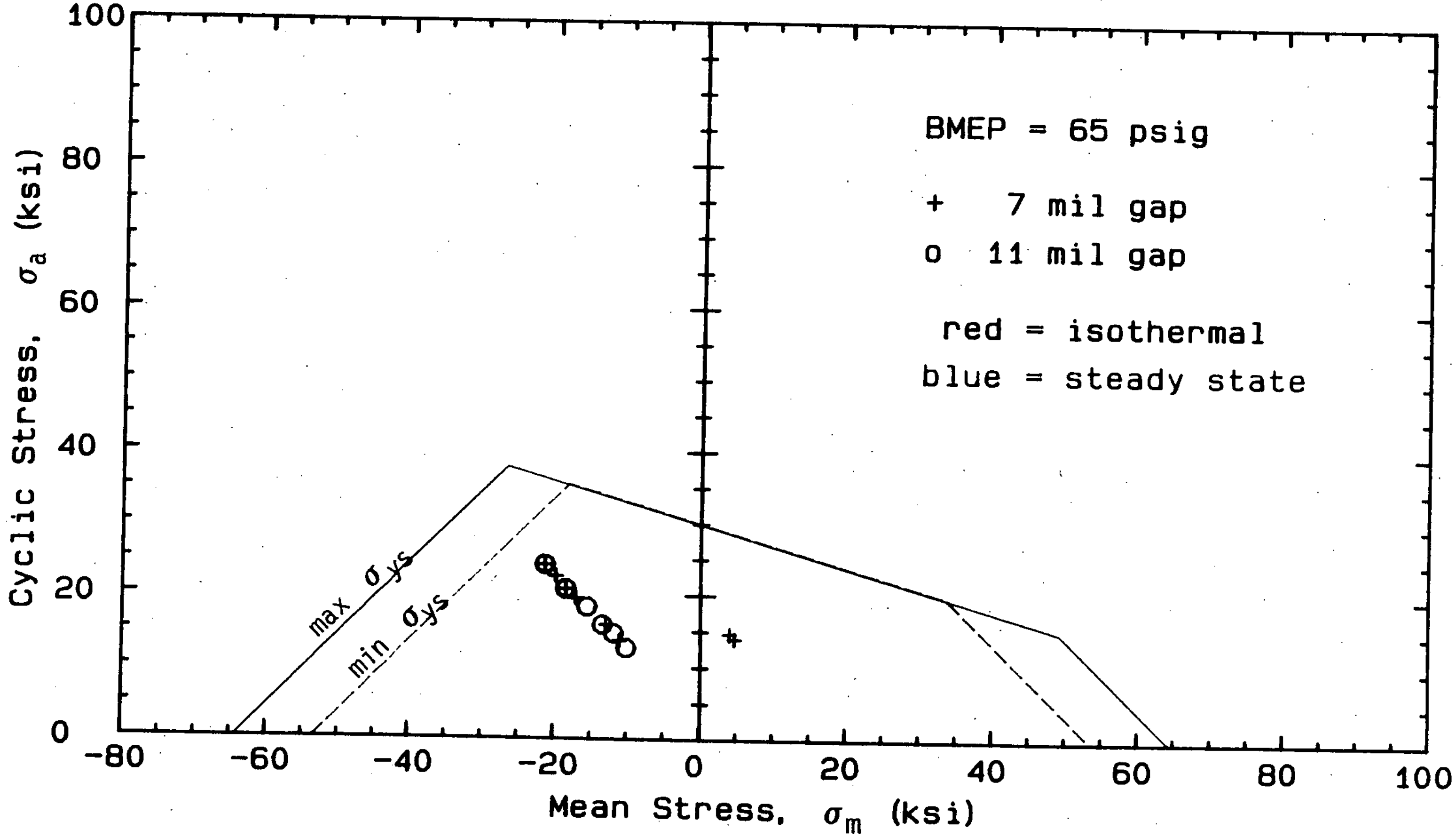

Figure 4-2. Mean and cyclic stresses at BMEP of psig along with Goodman diagram showing that cracks will not initiate at this BMEP. (Both min k and max k results shown.)

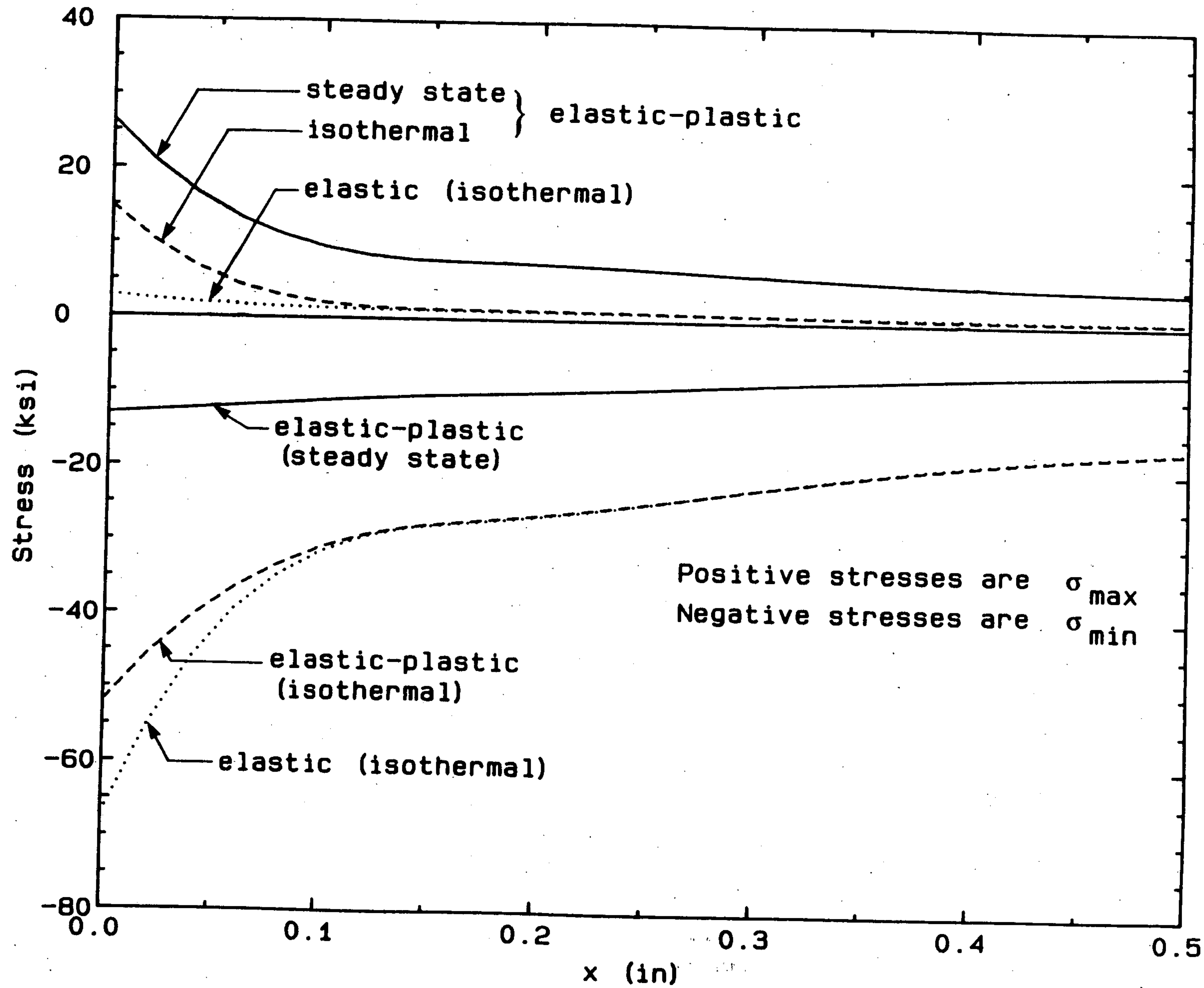

Figure 4-3. Elastic and elastic-plastic stresses as a function of depth into stud boss (experimental base line, 7 mil gap, max k).

FaAA-PA-R-88-06-15

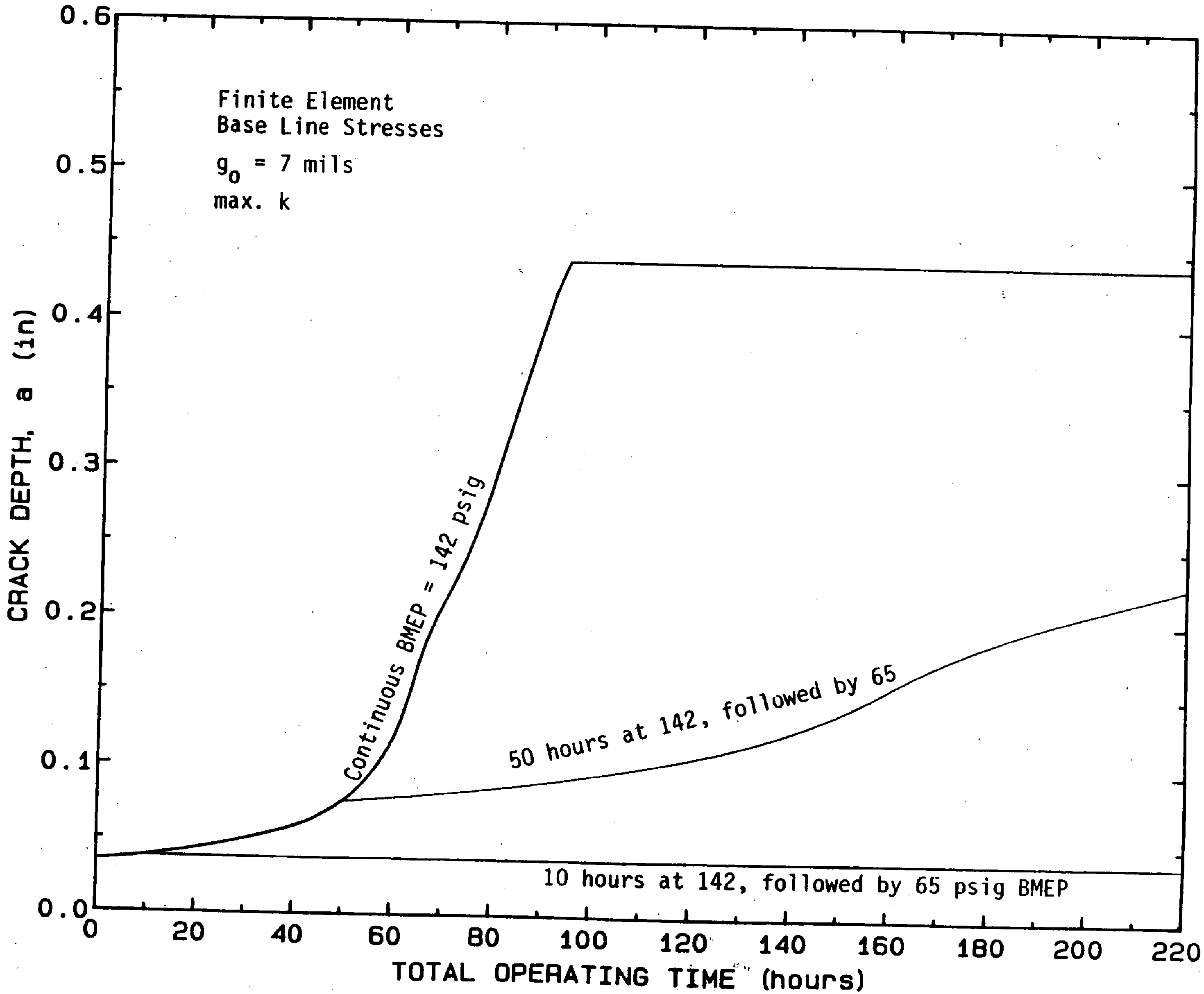

Figure 4-4. Crack depth as a function of time following exceedance of threshold conditions for three engine operation scenarios.

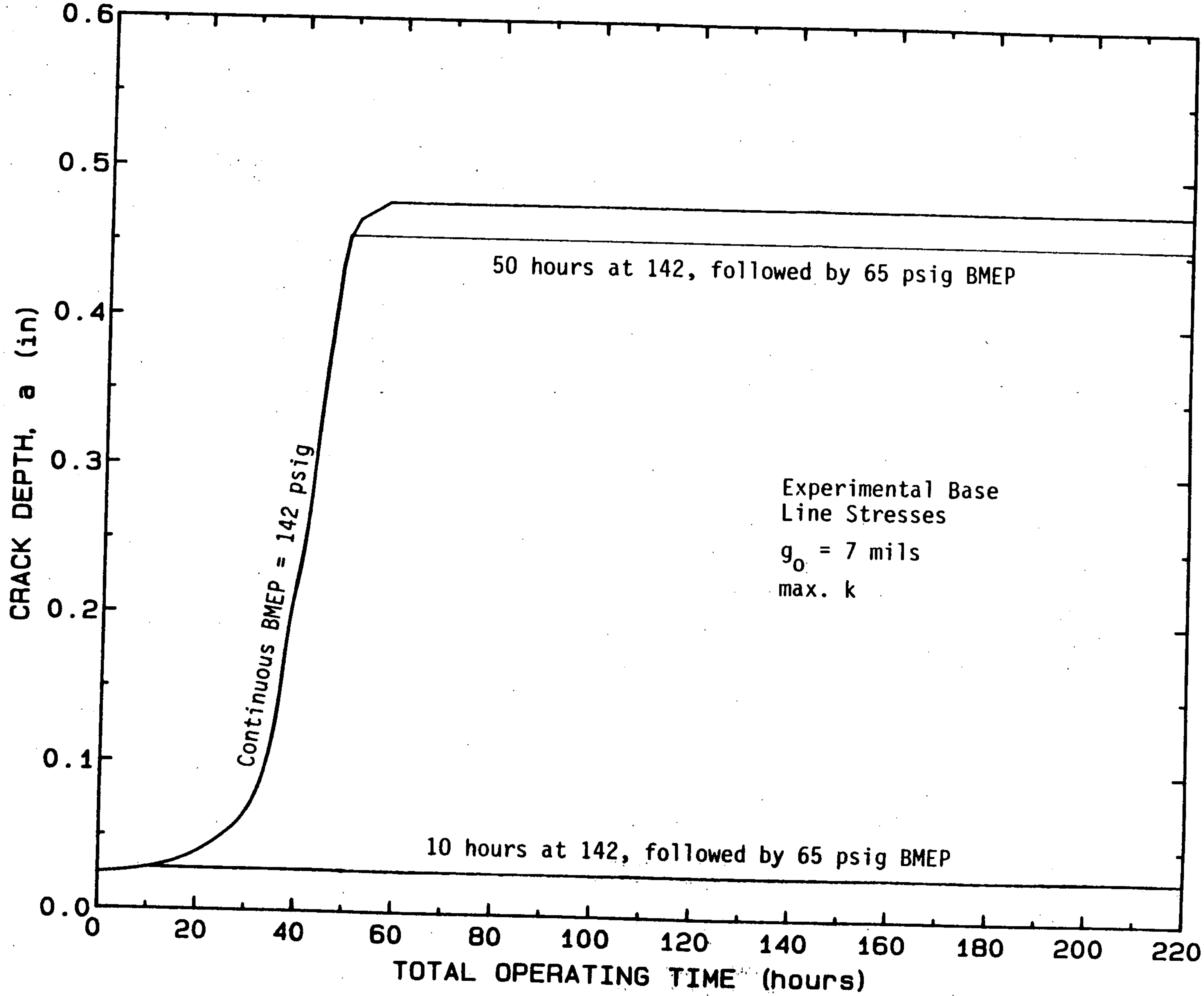

Figure 4-5. Crack depth as a function of time following exceedance of threshold conditions for three engine operating scenarios.

DESCRIPTION OF SUPPLEMENTAL CHANGES TO PROPOSED CHANGE NO. 190 TO THE TECHNICAL SPECIFICATIONS PROVISIONAL OPERATING LICENSE NO. DPR-13

The following is a supplemental request to revise Section 4.4, "Emergency Power System Periodic Testing," and 1.0, "Definitions" of the Appendix A Technical Specifications for the San Onofre Nuclear Generating Station, Unit 1 (SONGS 1).

DESCRIPTION OF SUPPLEMENTAL CHANGES

As a result of conversations and meetings with the NRC to discuss Proposed Change No. 190 (Amendment Application No. 153), the following additional changes are proposed:

1. Provide definitions for diesel generator "SLOW START" and "FAST START."

2. Specify that monthly diesel generator surveillance testing be performed by "slow" starting the diesel generators.

3. Specify that the 18 month diesel generator surveillance testing be performed by "fast" starting the diesel generators.

4. Require that the monthly surveillance test of the diesel generators be performed for the majority of the test at 4500 kW ± 5% load, and for a brief period of time at the new peak load of 5250 kW ± 5%.

PROPOSED TECHNICAL SPECIFICATIONS

See Attachment 1

SIGNIFICANT HAZARDS CONSIDERATION ANALYSIS

The analysis provided by Amendment Application No. 153 bounds the additional conditions proposed herein. The additional conditions provide restrictions that limit the stresses placed on the diesel generator during surveillance testing resulting from the increased loading limit proposed by Amendment Application No. 153. Therefore, the additional conditions proposed herein are determined to be more conservative and the significant hazards consideration analysis contained in Amendment Application No. 153 remains bounding.

It is noted that SCE previously proposed Technical Specification changes to incorporate definitions and testing stipulations for diesel generator "slow starts" and "fast starts." These changes were proposed by Amendment Application No. 126 submitted by SCE's letter dated February 14, 1985. This aspect of SCE's application has not been approved by the NRC. The supplemental changes proposed herein regarding "slow starts" and "fast starts" are essentially the same as those previously submitted. The only significant deviation is that the "slow start" proposed herein requires that the diesel generator achieve operating frequency and voltage in not less than 24 seconds versus greater than 10 seconds as previously proposed. In the event that "slow start" surveillance testing of the diesel generators inadvertently achieves steady state frequency and voltage in less than 24 seconds, the surveillance will not be considered a failure. Thus, failure to satisfy this aspect of the surveillance testing will not require re-starting the diesel generators.

The proposed requirement to test the diesel generators at 5250 kW ± 5% for a "brief" period of time is proposed in order to subject the diesel generators to the maximum possible loads for a short duration in order to verify the ability to function with the higher load. The probability of an event inducing the combination of conditions necessary to result in the maximum load is very low. Consequently, a brief duration for this test, expected to be approximately three to five minutes, was determined to adequately demonstrate the ability of the diesel generators to function at this load while minimizing the increased stresses at this higher load.

SAFETY AND SIGNIFICANT HAZARDS CONSIDERATION DETERMINATION

Based on the Safety Evaluations provided in Amendment Application No. 151 and Amendment Application No. 126, and the information provided above, it is concluded that: (1) the supplemental changes to Proposed Change No. 190 do not involve a significant hazards consideration as defined by 10 CFR 50.92; and (2) there is reasonable assurance that the health and safety of the public will not be endangered by the proposed change.

Attachment 1 - Supplemental Changes to the Proposed Specifications

MJT:0083n

ATTACHMENT 1

SUPPLEMENTAL CHANGES TO

PROPOSED CHANGE NO. 190

CORE ALTERATION

1.6 CORE ALTERATION shall be the movement or manipulation of any component within the reactor pressure vessel with the vessel head removed and fuel in the vessel. Suspension of CORE ALTERATION shall not preclude completion of movement of a component to a safe conservative position.

CORRELATION CHECK

1.7 A CORRELATION CHECK shall be an engineering analysis of an incore flux map wherein at least one point along the incore versus excore correlation data plot is obtained.

CORRELATION VERIFICATION

1.8 A CORRELATION VERIFICATION shall be the engineering analysis of incore flux maps wherein multiple points along the incore versus excore correlation data plot are obtained.

DG FAST START

1.8.1 DG FAST START shall be an automatic or manual start of an emergency diesel generator in which the steady state voltage and frequency is achieved within 10 seconds.

DG SLOW START

1.8.2 DG SLOW START shall be an automatic or manual start of an emergency diesel generator in which steady state voltage and frequency is achieved in not less than 24 seconds.

DOSE EQUIVALENT I-131

1.9 DOSE EQUIVALENT I-131 shall be that concentration of I-131 (microcurie/gram) which alone would produce the same thyroid dose as the quantity and isotopic mixture of I-131, I-132, 1-133, I-134, and I-135 actually present. The thyroid dose conversion factors used for this calculation shall be those listed in Table III of TID-14844, "Calculation of Distance Factors for Power and Test Reactor Sites."

FIRE SUPPRESSION WATER SYSTEM

1.10 A FIRE SUPPRESSION WATER SYSTEM shall consist of a water source(s), pump(s), and distribution piping with associated isolation valves (i.e., system header, hose standpipe and spray header isolation valves).

FREQUENCY NOTATION

1.11 The FREQUENCY NOTATION specified for the performance of Surveillance Requirements shall correspond to the intervals defined in Table 1.1.

4.4 EMERGENCY POWER SYSTEM PERIODIC TESTING

APPLICABILITY: Applies to testing of the Emergency Power System.

OBJECTIVE: To verify that the Emergency Power System will respond promptly and properly when required.

SPECIFICATION:

A. The required offsite circuits shall be determined OPERABLE at least once per 7 days by verifying correct breaker alignments and power availability.

B. The required diesel generators shall be demonstrated OPERABLE:

1. At least once per 31 days on a STAGGERED TEST BASIS by:

   a. Verifying the diesel performs a DG SLOW START from standby conditions,

   b. Verifying a fuel transfer pump can be started and transfers fuel from the storage system to the day tank,

   c. Verifying the diesel generator is synchronized and running at 4500 kW ± 5% for ≥ 60 minutes, to include a brief load increase to 5250 kW ± 5%,

   d. Verifying the diesel generator is aligned to provide standby power to the associated emergency buses,

   e. Verifying the day tank contains a minimum of 290 gallons of fuel, and

   f. Verifying the fuel storage tank contains a minimum of 37,500 gallons of fuel.

2. At least once per 3 months by verifying that a sample of diesel fuel from the required fuel storage tanks is within the acceptable limits as specified by the supplier when checked for viscosity, water and sediment.

C. AC Distribution

1. The required buses specified in Technical Specification 3.7, Auxiliary Electrical Supply, shall be determined OPERABLE and energized from AC sources other than the diesel generators with tie breakers open between redundant buses at least once per 7 days by verifying correct breaker alignment and power availability.

E. The required Safety Injection System Load Sequencer shall be demonstrated OPERABLE at least once per 31 days on a staggered test basis, by simulating SISLOP* conditions and verifying that the resulting interval between each load group is within ± 10% of its design interval.

F. The required diesel generators and the Safety Injection System Load Sequencer shall be demonstrated OPERABLE at least once per 18 months during shutdown by:

1. Subjecting the diesel to an inspection in accordance with procedures prepared in conjunction with its manufacturer's recommendations for this class of standby service.

2. Simulating SISLOP*, and:

   a. Verifying operation of circuitry which locks out non-critical equipment,

   b. Verifying the diesel performs a DG FAST START from standby condition on the auto-start signal, energizes the emergency buses with permanently connected loads and the auto connected emergency loads** through the load sequencer (with the exception of the feedwater, safety injection, charging and refueling water pumps whose respective breakers may be racked-out to the test position) and operates for $\geq$ 5 minutes while its generator is loaded with the emergency loads,

   c. Verifying that on the safety injection actuation signal, all diesel generator trips, except engine overspeed and generator differential, are automatically bypassed.

3. Verifying the generator capability to reject a load of 3220 kW without tripping.

* SISLOP is the signal generated by coincident loss of offsite power (loss of voltage on Buses 1C and 2C) and demand for safety injection.

** The sum of all loads on the engine shall not exceed 5250 kW + 5%.

Basis: The normal plant Emergency Power System is normally in continuous operation, and periodically tested.[1]

The tests specified above will be completed without any preliminary preparation or repairs which might influence the results of the test except as required to perform the DG SLOW START test set forth in T.S. 4.4.B.1.a. The tests will demonstrate that components which are not normally required will respond properly when required. Test loading of the generator to 4500 kW and 5250 kW corresponds to approximate engine brake mean effective pressures of 116 psi and 135 psi, respectively.

DG SLOW STARTS are specified for the monthly surveillances in order to reduce the cumulative fatigue damage to the engine crankshafts to levels below the threshold of detection under a program of augmented inservice inspection. In the event that the DG SLOW START inadvertently achieves steady state voltage and frequency in less than 24 seconds, the surveillance will not be considered a failure and require restart of the diesel generator.

The monthly surveillance specified by T.S. 4.4.B.1.c includes a "brief" load increase to 5250 kW ± 5%. This requirement verifies the ability to function under the maximum possible loading conditions. A "brief" test is required to demonstrate operability while minimizing the increased stresses from the higher load. The duration of this test is expected to be approximately three to five minutes.

The surveillance requirements for demonstrating the OPERABILITY of the station batteries are based on the recommendations of Regulatory Guide 1.129, "Maintenance, Testing, and Replacement of Large Lead Storage Batteries for Nuclear Power Plants," February 1978, and IEEE Std 450-1980, "IEEE Recommended Practice for Maintenance, Testing, and Replacement of Large Lead Storage Batteries for Generating Stations and Substations."

Verifying average electrolyte temperature above the minimum for which the battery was sized, total battery terminal voltage on float charge, connection resistance values and the performance of battery service and discharge tests ensure the effectiveness of the charging system, the ability to handle high discharge rates and compares the battery capacity at that time with the rated capacity.

Table 4.4-1 specifies the normal limits for each designated pilot cell and each connected cell for electrolyte level, float voltage and specific gravity. The limits for the designated pilot cells float voltage and specific gravity, greater than 2.13 volts and .020 below normal full charge specific gravity or a battery charger current that has stabilized at a low value, is characteristic of a charged cell with adequate capacity. The normal limits for each connected cell for float voltage and specific gravity, greater than 2.13 volts and not more than .020 below normal full charge specific gravity with an average specific gravity of all the connected cells not more than .010 below normal full charge specific gravity, ensures the OPERABILITY and capability of the battery.

Operating with a battery cell's parameter outside the normal limit but within the allowable value specified in Table 4.4-1 is permitted for up to 7 days. During this 7 day period: (1) the allowable values for electrolyte level ensures no physical damage to the plates with an adequate electron transfer capability; (2) the allowable value for the average specific gravity of all the cells, not more than .020 below normal full charge specific gravity, ensures that the decrease in rating will be less than the safety margin provided in sizing; (3) the allowable value for an individual cell's specific gravity, ensures that an individual cell's specific gravity will not be more than .040 below normal full charge specific gravity and that the overall capability of the battery will be maintained within an acceptable limit; and (4) the allowable value for an individual cell's float voltage, greater than 2.07 volts, ensures the battery's capability to perform its design function.

Reference: (1) Supplement No. 1 to Final Engineering Report and Safety Analysis, Section 3, Questions 6 and 8.